COMPENSATION OF PHOTOBLEACHED IMAGES FOR A CELL DYNAMICS SYSTEM

by

SOWMYA GOPINATH

Presented to the Faculty of the Graduate School of

The University of Texas at Arlington in Partial Fulfillment

of the Requirements

for the Degree of

MASTER OF SCIENCE IN COMPUTER SCIENCE AND ENGINEERING

THE UNIVERSITY OF TEXAS AT ARLINGTON

December 2006

Dedicated to my friends and family.

ACKNOWLEDGEMENTS

I would like to thank my thesis advisor, Dr. Jean Gao and my colleague Ninad Thakoor for their invaluable guidance throughout my research. I am grateful to Quan Wen and Jiaxing Xue for their suggestions and support in the design of Intracellular Dynamic Analysis System (ICellDAS) interface. I would also like to thank Dr. Hua-mei Chen and Dr. Nan Zhang for presiding in my defense committee.

Finally I thank my friends and family for supporting me in this endeavor.

November 22, 2006

ABSTRACT

COMPENSATION OF PHOTOBLEACHED IMAGES FOR A CELL DYNAMICS SYSTEM

Publication No. _____

Sowmya Gopinath, M.S

The University of Texas at Arlington, 2006

Supervising Professor: Jean Gao

Progress in the field of medicine attributes to the discoveries in biology that require an extensive knowledge of cell dynamics. Intracellular Cell Dynamics Analysis System (ICellDAS) is a web based tool aimed at automating sub cellular particle motion estimation, tracking and mobility analysis. The purpose of this tool is to develop a better understanding of specific biology problems by visualizing biological data. For reliable analysis as well as visualization of cell dynamics, it is essential that the acquired images reflect the exact information of the specimen. The goal of the thesis is to design an interface for the ICellDAS project and to develop a method to compensate the information loss in photobleached images. Photobleaching is the irreversible destruction of fluorescence within the stained specimen caused due to scattering, absorption of

excitation and fluorescence light in a confocal laser scanning microscope. Current approaches to solve this problem are computationally complex, time consuming, restricted to exponential decay model and highly sensitive to noise. The proposed method provides a simple yet effective statistical approach to solve this problem. It aims to overcome the disadvantages of current methods and at the same time provides better visualization of photobleached images. The main idea is to filter the foreground information from a given image by modeling it as a mixture of Gaussians and use this information to compensate the intensity loss of the photobleached images. The experimental results show that the restored images have better contrast and visual value compared to the original stack of photobleached images. The interface for ICellDAS is designed based on the design principles and philosophies for web application development. The interface has helped to identify various constraints such as speed, memory limitations, and security of the images which should be addressed for the success of ICellDAS project.

TABLE OF CONTENTS

LIST OF ILLUSTRATIONS

CHAPTER 1

INTRODUCTION

Unraveling the mysteries of cell has helped mankind to make remarkable progress for a better understanding of mystery of life. In the field of cell biology voluminous data is collected. The need to interpret such a large amount of data requires tools that are in the realm of computer science. These tools often involve algorithms to provide the correct estimates of different aspects of data which is of the central importance to theoretical computer science. Biologists need reliable tools to deal with huge amount of data at the touch of a key or a click of the mouse.

Today, the use of Web has become an integral part of teaching and learning methodologies. A number of application programs are made available through the internet. The vast number of daily visits to some of the genomic sites such as National Institutes of Health (NIH) proves that the internet has become the hub for sharing and learning various aspects of cell biology. Keeping these aspects in mind, Intracellular Dynamics Analysis System (ICellDAS) was proposed by the Biocomputing and Vision lab at University of Texas, Arlington, headed by Dr. Jean Gao in the year 2005. The goal of the proposed system is to develop a unique and first web based open access system for automating sub cellular particle motion estimation, tracking and mobility analysis. It also aims to integrate all the tools required for qualitative analysis of medical images and provide practical hands on experience to the learning community of

cell biology. In this thesis, we have proposed one such image processing tool "De-photobleaching", to help in the qualitative analysis of images acquired by confocal microscopies.

For more than a century, microscope is used as a research tool to reveal cellular structure and to explore the properties of cell. In the 1800, microscope was no more than a simple lens system of higher resolution. At the turn of the twentieth century, Kóhler illumination revolutionized the bright field microscopy. Later developments in the illumination techniques such as phase-contrast illumination, Normaski illumination and epi-illumination had significant impact on microscopy [1]. The advent of confocal microscopy brought it to the forefront of research in cell biology. It has changed the way specimens were prepared and examined. Using this technology, biologists can precisely locate labeled molecules in specimens. But just as any other technique, confocal microscopy has its own set of disadvantages. One among them is the bleaching of the acquired image due to the destruction of fluorophores (markers) by a process called photobleaching. The bleached images represent blurred objects. Hence a qualitative analysis of the object is not possible without correcting the loss in intensity. Current approaches to solve this problem are either computationally complex, time consuming, restricted to exponential decay model or highly sensitive to noise. In this thesis, we present a simple but effective statistical method to correct the intensity loss in photobleached image. In addition to this work, an initial interface for the proposed ICellDAS has been developed.

In chapter 2, a literature review of confocal microscopy is provided. It discusses the working principle of confocal microscope and how it differs from conventional fluorescence microscope, the factors that affect the confocal image formation. It also gives a brief account on the advantages and disadvantages of this technique. The chapter ends with an account of the different applications of confocal microscopy.

In chapter 3, we first give a detailed description of the photobleaching process. Then we propose a Gaussian mixture model based approach to correct the intensity loss in photobleached images. The correction algorithm is explained in detail along with a brief account of previous work on this topic. Finally, we present our experimental results. To evaluate the performance of our proposed method, we compare the mean intensities of all the sections in the image stacks before and after correction. The mean intensity curves are presented at the end of chapter.

In chapter 4, we discuss the philosophies and principles followed while designing the interface for ICellDAS. We also present a brief report on the tools used for design and development.

Finally, we conclude this work in chapter 5 with some discussion and suggested future work.

CHAPTER 2

CONFOCAL MICROSCOPY

Confocal laser scanning microscope is a light microscopial imaging technique which has gained wide popularity in biological sciences. In this chapter we present theoretical concept of confocal microscopy. In section 2.1, a brief history of confocal microscope is presented. Section 2.2 explains the phenomenon of fluorescence. Section 2.3 and 2.4 explain the working principle of fluorescence and confocal microscope. Section 2.5 elucidates two design types of fast confocal microscope. Section 2.6 contains a brief introduction of three dimensional visualization of confocal microscopy. The advantages and limitations of confocal microscope is discussed in section 2.7 and 2.8 respectively. The chapter ends with applications of confocal microscope.

2.1 Background of Confocal Microscope

Confocal microscope was an important invention of the eighties since it offered observation of optical sections in thick intact specimens. It was invented by Marvin Minsky in 1955 while he was a junior fellow at Harvard University. The term confocal refers to the state where two lenses are arranged such that, they focus on the same point. Confocal microscope helped produce image of unprecedented quality by avoiding unwanted scattered light that clouds an image when the entire specimen is illuminated at the same time. The “out of focus” light is removed by means of a confocal pinhole placed in front of the image plane which acts as a filter that allows only the in-focus

portion of the light to be imaged. Minsky's model was commercially unfeasible at that time due to lack of technology such as intense light source and computer horse power to produce useful images. Later in 1986-87, Brad Amos and John White of Cambridge University constructed the first commercial confocal microscope by combining the technologies of the laser, computer and microelectronics. During the 1990's, advances in optics and electronics such as stable and powerful lasers, high-efficiency scanning mirrors, high-throughput fiber optics, better thin film dielectric coatings and detectors with reduced noise characteristics set stage for the boom in the number of applications that could use Confocal Laser Scanning Microscope (CLSM) [2]. Modern Confocal microscopes have kept the key elements of Minsky's prototype such as pinhole apertures and point by point illumination of the specimen except for added features such as automated control of laser brightness, improved image quality and increased storage capacity for the generated images. Confocal microscopes can be categorized into those that image by reflecting light off the specimen or by stimulating fluorescence from the dyes applied to the specimen. Fluorescence confocal microscopy is the most commonly used mode in biological applications and hence is the subject of our study.

2.2 Fluorescence

Fluorescence is defined as the radiative transition between two electronic states of the same spin multiplicity [3]. When an atom or a molecule absorbs light, each quantum taken up by the atom or the molecule interacts with it to promote an electron from lower energy to higher energy molecular orbit. According to Neil Bohr's theory of atomic and molecular structure, an atom or a molecule can exist only in a series of

discrete states of electronic energy. The lowest energy level is the ground state E_0, where an atom or molecule exists in the absence of external activation. E_1 and E_2 are the higher energy levels where an atom or molecule can exist only in a excited state. By absorbing light energy, the electrons within an atom increase their energy causing it to jump to a discrete singlet excited state [4]. Each electronic state has a number of vibrational levels superimposed on it. The vibrational levels are brought on; in molecules of a given electronic state which may absorb small increments of energy corresponding to the changes in vibrational modes at the same time retain the same electronic configuration. The time taken for photon absorption is approximately 10^{-5} seconds and is faster than molecular vibrations. Hence the molecule maintains its internuclear geometry before and after absorption to form the excited state. This is the Frank Condon principle [3].

Depending on the environment, an excited molecule can either emit a photon from the same vibrational level to which it was excited initially or undergo changes in vibrational levels prior to emission of radiation. This generation of luminescence is termed as photoluminescence, which is formally divided into two categories depending on the electronic configuration of the excited state and the emission pathway. If the excited atom or molecule emits light of longer wavelength after its lifetime which is approximately 10^{-9} to 10^{-7} seconds, the process is termed as fluorescence. The quantum of radiation emitted in fluorescence is lower in energy on average than the quantum absorbed by the molecule due to vibrational relaxation which occurs both after absorption and after emission. This change in light energy causes a shift of the

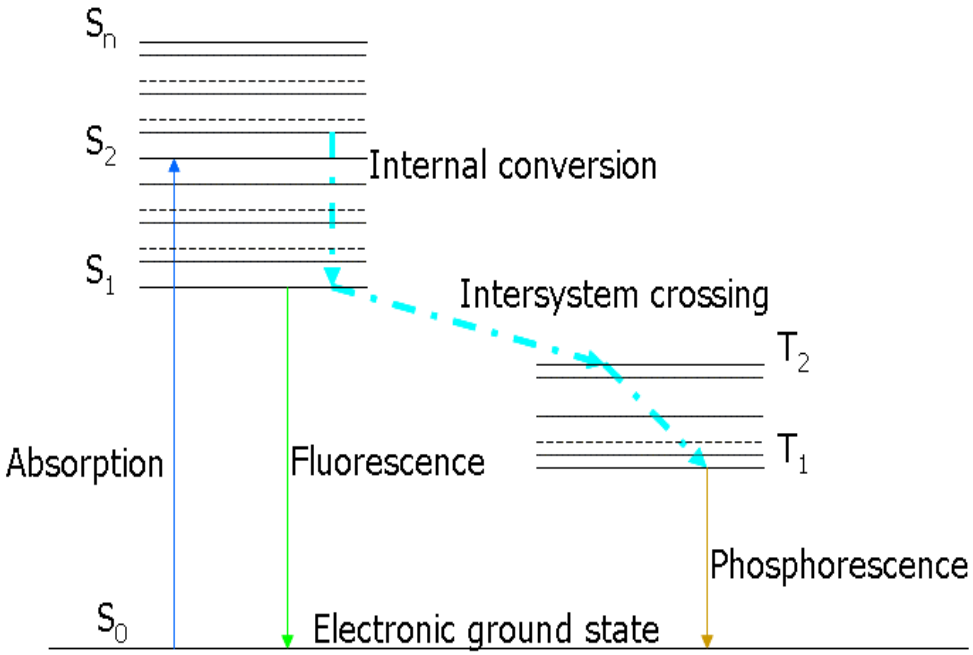

Figure 2.1 Jablonski Energy Diagram [5]

fluorescence spectrum to longer wavelength, relative to absorption spectrum and is termed as the Stokes shift. The process of phosphorescence occurs in a way similar to fluorescence, but has a much longer excited lifetime than fluorescence. Phosphorescence occurs when a molecule is placed in a rigid medium with less collisional processes and is characterized by an after glow which is not observed in fluorescence. One of the most important applications of fluorescence in cell biology is live cell imaging. The ability to observe processes as they occur is vital to the understanding of cell functions. Fluorescein is a common fluorophore (also referred to as chromophore, are components of molecules which absorb light) which emits green light when stimulated with blue excitation light. The wavelength and color of the

excited light is dependent on material. Fluorescent dye molecules can be attached to specific parts of the specimen which is required to be observed. More than one type of fluorophore can be attached and by changing the excitation light, different parts of the specimen can be studied.

2.3 Working Principle of Fluorescence Microscope

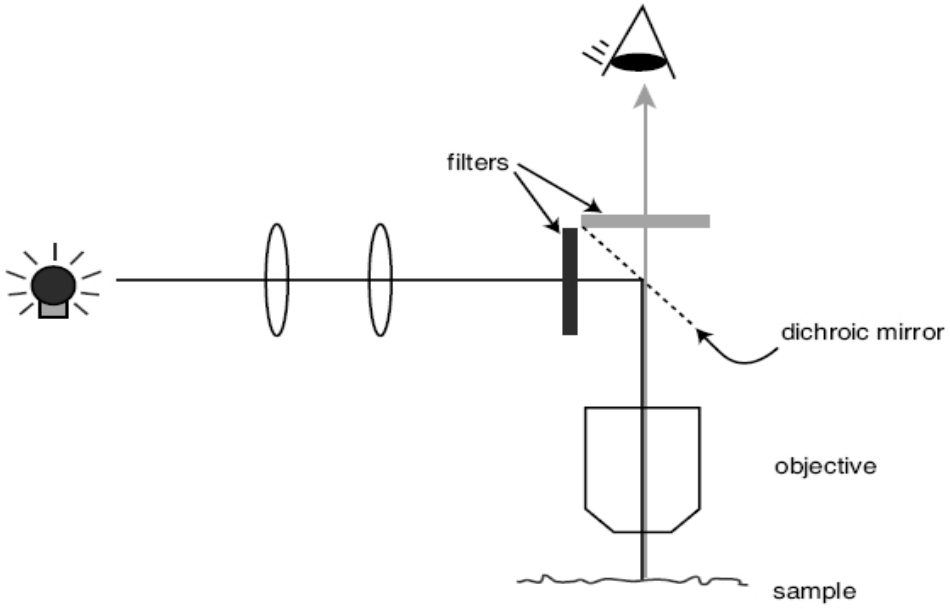

Figure 2.2 Principle of a Fluorescence Microscope [6]

In conventional fluorescence microscope, a high intensity light is used to illuminate a stained specimen. The image is formed by the fluorescent light emanating from the stained parts of the specimen. A dichroic mirror which reflects light, shorter than a certain wavelength but transmits light of longer wavelength is used for this purpose (Figure 2.2). The light from the main source passes through the objective lens,

dichroic mirror and a barrier filter (which eliminates light of different wavelength other than fluorescent). This optical set up which uses objective lens to focus light (illuminating light and fluorescent light) to and from the specimen is called epi-fluorescence [6].

2.4 Working Principle of Confocal Microscope

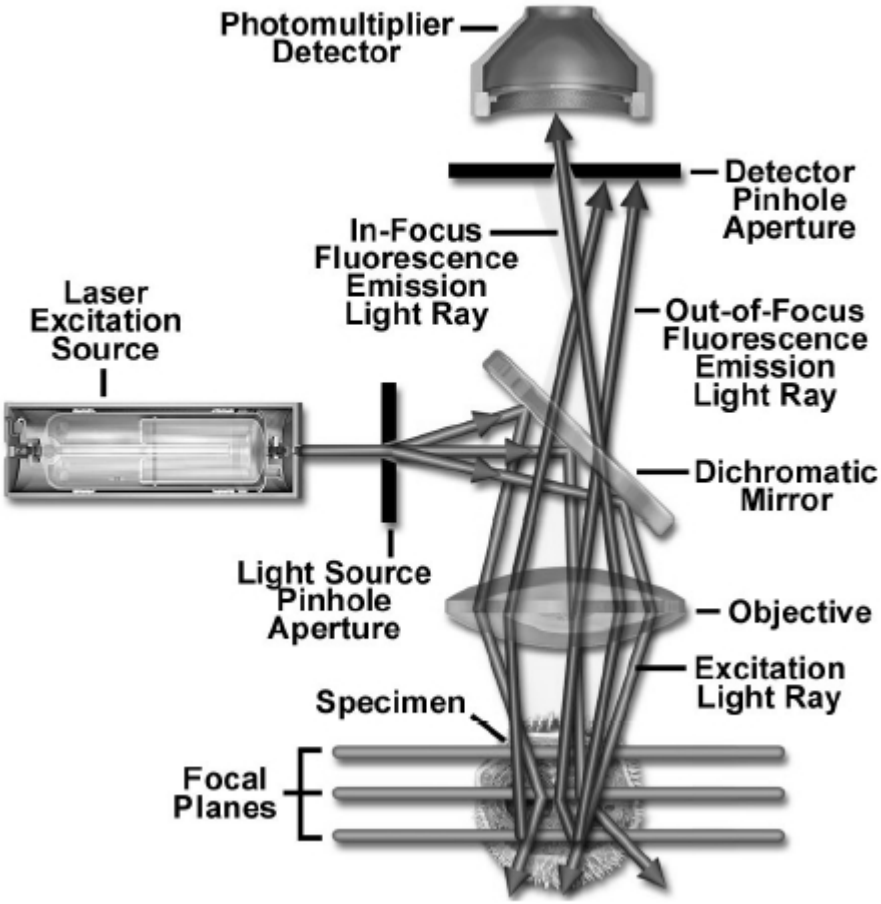

Figure 2.3 Principle of a Confocal Microscope [7]

The confocal microscope rejects out-of-focus light by using the technique of point-by-point illumination of the specimen. The drawback of imaging a point at a given time is that a fewer photons are emitted at that point. Hence, there is less information to collect. This will increase the noise factors associated with the image. The noise can be avoided by illuminating each point for a longer time, to collect sufficient light to make an accurate measurement. Using ordinary source of light increases the time frame to produce a point by point image. This can be avoided by using a high intensity light source like laser. By using laser as the illuminating light source, one can take advantage of its wide range of wavelength required to excited different kinds of fluorescent dyes.

Light emitted from the excitation source passes through a pin hole aperture and reflects off a dichroic mirror, which directs it to the specimen through an assembly of vertical and horizontal mirrors. The mirrors help to scan the laser across the specimen. A second pinhole aperture is placed in front of the detector such as a photomultiplier tube. The stained specimen excited by high intensity laser fluoresces. The fluorescent light emitted from the specimen passes back through the dichromatic mirror and focuses as a confocal point at the detector pinhole aperture. The extraneous light (termed out-of-focus light) is blocked by the pinhole aperture and is not detected by the photomultiplier. The dichroic mirror, filter performs the same functions as in a wide field epi-fluorescence microscope.

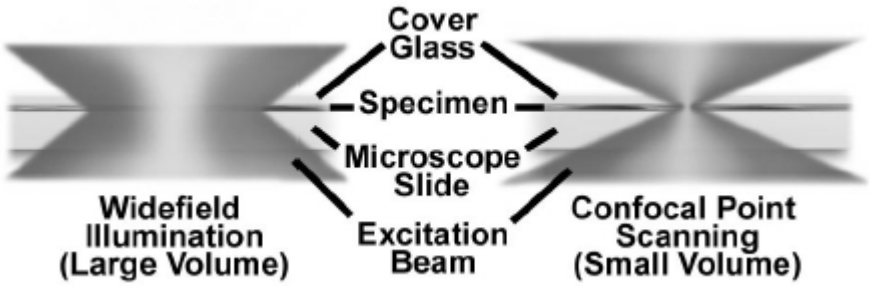

Figure 2.4 Widefield Vs Confocal Microscope Illumination Volumes [7]

The only difference is that confocal microscope shifts the excitation and emission points on a specimen to a new plane which is confocal with the pinhole aperture of the light source and the detector (Figure 2.4). Since confocal microscope images only one point at any given instant, a computer which builds up the image one pixel at a time is attached to the detector for the purpose of investigation of the acquired images.

2.4.1. Image Formation:

The most common method to acquire confocal image is by scanning the laser beam over the object using a pair of galvanometer mirrors. One galvanometer scans in the x direction while the other in the y direction. The fluorescence light is collected by photomultiplier (converts it to analog signal) and fed to Analog to Digital Convertor (ADC) which displays the signal as a sequential raster scan of the image. Based on the desired measurements (within the limits of imaging requirement), scan ranges from 50×50 up to 4096×4096 points can be collected. The most widely collected scan size is 512×512 points based on the fastest possible point scanning available on the instrument. On selecting the image area, the image collection parameters can be adjusted according to the required resolution. Electronic magnification is one of the most useful features of

confocal microscopy. According to the principle of electronic magnification, the number of pixels in the collected area remains constant as the imaging area is reduced. However an image can be magnified only within the limits of Nyquist criterion. The power delivered to the specimen is directly proportional to the square of the magnification. Hence magnification beyond reasonable limits is harmful to the specimen or could aggravate the rate of photobleaching.

2.5 Fast Confocal Microscopy

A simple confocal microscope takes 0.1 to 1 second to generate a single image [6]. This speed is too slow to capture dynamic events that occur in the specimen. Two commonly used designs to capture high speed images are the Nipkow disk confocal microscope and acousto-optic deflector (AOD) confocal microscope.

2.5.1. Acousto-Optic Deflector Confocal Microscope:

The speed of confocal microscope is limited by the galvanometer mirrors that scan along the vertical and horizontal directions [6]. The usual working is a slow scan in the vertical direction combined by a rapid scan in the horizontal direction. AOD helps to increase the speed of horizontal scan. AOD is a device that deflects light by creating a diffraction grating out of crystal using high frequency sound waves. The high frequency sound waves acts as pressure waves and alters the refractive index of the crystal. Thus when a light source passes through the crystal, it is deflected at an angle based on the frequency of acoustic pressure waves. By controlling the frequency of sound waves, the angle of deflection of light source can be varied. The disadvantage of AOD confocal microscope is that AOD is wavelength specific (fluorescent emission of

longer wavelength cannot be scanned by the AOD). One way to solve this problem is to partially scan along the vertical direction (controlled by slow galvanometer) and collect the light using a slit instead of a pinhole [8]. The resulting images are confocal along one axis and slightly distorted. Yet they are applicable to certain applications if not all.

2.5.2. Nipkow Disk Confocal Microscope:

Nipkow disk is a mechanically spinning disk, with a series of equally distanced circular holes of equal diameter drilled in it. Excitation light passes through the holes of the disk instead of pin hole aperture, thereby illuminating many discrete points simultaneously. At any given time only a small section of disk is illuminated. The returning light (fluorescence emission) also passes through the same pinholes for optical sectioning. As the disks spin, the entire specimen is covered several times in a rotation. The disadvantage of Nipkow disk is that only ~1% of the illuminating light reaches the specimen [9]. This can result in a weak signal and poor imaging in fluorescence mode. However with strong fluorophores, images with the same quality as that of Confocal Laser Scanning Microscope can be obtained [9].

2.6 Three Dimensional Microscopy Visualization

Three dimensional visualization plays an important role in the study of cellular structures in biomedical research. Three dimensional renditions of the specimen are created from the optical sections produced by the confocal microscope. The data collected from several images taken along the z axis (termed as optical axis) of the specimen at regular intervals is put together to create 3D image. This way any living tissue can be visualized without doing physical harm to it by sectioning.

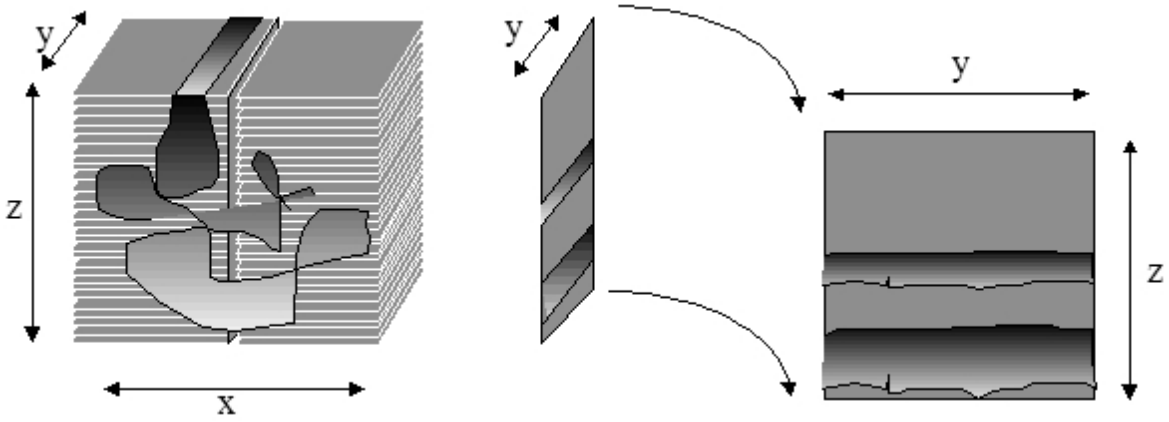

Figure 2.5 3D Visualization from Optical Sections of an Image Stack [10]

Additionally much information can be obtained on the structure of the specimen by looking at the sample from different view points. The power of computer is used for this process. Figure 2.5 shows how different optical sections of the specimen can be arranged to get a three dimensional view of the specimen. Several algorithms have been developed to retrieve information from 2D images which is used for construction of meaningful 3D images.

2.7 Benefits of Confocal Microscopy

Few advantages of confocal microscope over conventional fluorescence microscope are elucidated below [1]:

a) Effective resolution: The pin hole aperture of the microscope provides increased resolution.

b) Reduced blurring of acquired image: The pin hole aperture excludes "out-of-focus" light from image plane, thus creates sharper images than conventional fluorescence microscope.

c) Improved signal to noise ratio: As the background light is decreased in confocal microscopy, there is a significant improvement in the signal to noise ratio.

d) Z axis scanning: A series of optical sections is imaged at regular distance by moving the objective through the specimen from bottom to top.

e) Depth perception: The reconstruction of acquired image can be done along the entire depth of the specimen.

f) Magnification adjustment: Confocal microscopy has provided the capability to magnify the image electronically by reducing the scanned area under excitation source, at the same time maintaining the effective resolution of the object.

2.8 Limitations of Confocal Microscopy

Confocal microscopy, like any other technique is not a perfect technology. It has its own set of advantages as well as disadvantages. To make good use of its capabilities, it is required to have a good understanding of its limitations [6]. Some of the important considerations of a confocal microscope are:

a) Resolution: The resolution of the confocal microscope is limited by factors such as wavelength of illuminating light, diffraction effects. A confocal microscope does not resolve better than about 0.1 microns under ideal conditions [11]. Objects smaller than this resolution has to be visualized by using appropriate dyes. The extraneous emission (termed out-of-focus light rays) forms an extended airy disk in the aperture plane. These

airy disks limit the maximum resolution that can be attained with the confocal microscope. Resolution along the optical axis is also limited by diffraction effects.

b) Pinhole size: Optical sectioning would not have been capable without the pinhole aperture component of the confocal microscope. At the same time it should be noted that as the pinhole size is reduced, the number of photons that arrive from the specimen is reduced. This leads to a reduced signal to noise ratio. One solution to this problem is use a high intensity light for excitation but high intensity light can be harmful to certain specimens.

c) Photo damage: The high intensity light such as laser, when focused onto a fine spot on the sample can damage both the dye and the specimen. This photo damage can be controlled by using suitable anti fade reagents, however anti fade work only for fixed cell preparations and may be toxic to live cells in certain cases.

d) Cost: Another limitation worth mentioning is the cost of the instrument. Confocal microscopes are quite expensive instruments. Considerable amount of training of personnel, care and maintenance of the machine is required to gain maximum benefits from the confocal microscope.

2.9 Applications of Confocal Microscopy

The wide applications of confocal microscopy attributes to its ability to produce sharper images than the ones created by conventional wide field microscope by suppressing out-of-focus signals called as depth discrimination or optical sectioning. Some important applications of confocal microscopy [1] are:

a) Cell Biology: One of the important applications of confocal microscope is cell tracking using Green Fluorescent Protein (GFP). GFP is a fluorescent protein (naturally occurring in jelly fish) that acts as a reporter tool when transfected to living cells. It helps to track the presence of protein and for identifying regulatory genes in developmental biology.

b) Microscopy of living cells: A cell system with several fluorescent markers is studied by using the correlative tools of confocal microscopy.

c) Calcium Imaging: Phenomena such as changes in cellular PH, Ca^{2+} ions, membrane potential and oxidative processes within cells is evaluated by exciting them using a light source of single wavelength. The emitted light has two or more wavelengths based on the changes in the properties of the molecule.

d) Cell Adhesion studies: Confocal microscope has helped in the study of cell attachment and release mechanisms of human osteoblasts and in the study of chondrocytes in Vivo.

e) Co-localization: Confocal microscopy is considered as one of the best technologies to study co-localization (distribution of molecules produced within living organisms). Its ability to create accurate three dimensional structural representations of cells and organelles is the reason for its wide usage in cell biology.

f) Fluorescence recovery after photobleaching (FRAP): Photobleaching is a process where fluorophores fade irreversibly when exposed to excitation light (this process is explained in detail in next chapter). Quantities such as diffusion coefficient of the dyed structure can be determined by FRAP. A small portion of the specimen is exposed to

short and intense laser light. The laser beam destroys the local fluorescence of that spot. By observing the recovery of fluorescence in the bleached spot, dynamics of chemical changes that occur in the specimen is measured.

CHAPTER 3

DE-PHOTOBLEACHING FRAMEWORK

In this chapter, we present the proposed approach to solve the problem of intensity loss in photobleached images. Our objective is to develop a post processing method to correct the intensity loss due to fluorescence photobleaching in images acquired by confocal microscopy. In section 3.1, we explain the process of photobleaching. Section 3.2 gives a brief account of the previous work done to solve the problem of photobleaching. Section 3.3 explains the background of our proposed approach. We present proposed algorithm in section 3.4. The chapter ends with experimental results in section 3.5

3.1 Photobleaching

Fluorophore is one of the important aspects of Confocal microscopy (section 2.2). It bleaches over time due to exposure to excitation light. Though this process is not completely understood, one reason is the interaction of oxygen and/or oxygen radicals formed as a byproduct of the photochemistry of fluorescence with the fluorophore causes it to lose its capacity to emit fluorescence. This irreversible destruction of the fluorophore is called photobleaching. The photobleaching reaction takes place after the electrons of the fluorophore molecules undergo a spin conversion into the forbidden triplet state (T) instead of the lowest singlet state. This process is called as intersystem crossing. The triplet state has a longer span than the singlet state. During the longer

stay, the triplet state fluorophore population interacts with other molecules such as oxygen to produce irreversible covalent modifications. Figure 3.1 shows the difference between the fluorescence and bleaching process.

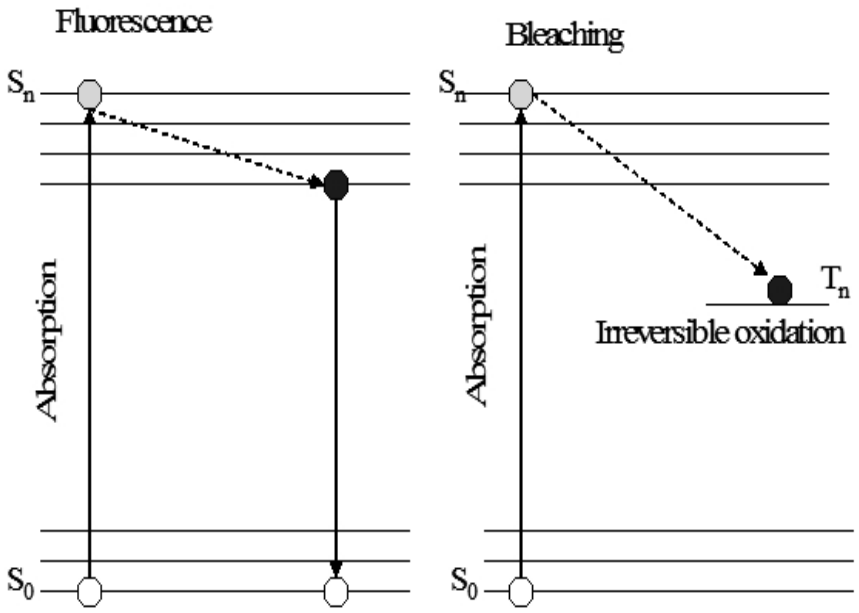

Figure 3.1 Jablonski Energy Diagram: Fluorescence and Photobleaching Process [19]

The rate of photobleaching is dependant on the molecular structure of the fluorophore and the local environment. Some fluorophores bleach after emission of a few photons while other robust fluorophores can undergo thousands or millions of excitation and emission cycles before bleaching. The rate of photobleaching can be reduced by a high numerical aperture lens which can collect more fluorescence and use less excitation light. The downside is low magnification (reduction in the intensity of excitation light by spreading it over a large cause low magnification).

3.2 Introduction to De-photobleaching

Fluorescent images produced by Confocal Laser Scanning Microscope (CLSM) tend to decrease in intensity with time or depth or both as an effect of photobleaching. Apart from photobleaching, there are many other factors such as signal to noise ratio and geometrical optics which affect the intensity of an image. The mechanisms and actual effects of these factors are very difficult to model for real observations [12]. These effects do not help to do a quantitative analysis of the image without correction. Methods used to compensate or correct this intensity loss can be categorized into two types

1) Pre-processing methods that correct the geometrical optics at the imaging stage.

2) Post-processing methods that model the loss in intensity for the purpose of correcting the bleached images.

We concentrate on post processing methods to correct the intensity loss. A lot of papers have been published which have focused on this problem and have given different approaches towards intensity variations correction. In [13], the authors apply a general model in which the flow field and additive and multiplicative intensity relationships are estimated at every pixel. This approach is time consuming [14]. Another approach is based on least square optimization with brightness and contrast set as optimized parameters [15, 16]. These techniques are highly sensitive to noise. In [16], reweighed least square method is used to correct the disadvantage of [15], but fails to correct the problem. The method discussed in [16] is not only sensitive to noise which can be

eliminated by median filtering but also to the dynamic movement of objects in neighboring optical sections which gives erroneous and unstable results even in the presence of low noise in optical sections [14]. In [17], intensity variations are corrected based on histogram warping, but it is restricted to the case where a global, spatially invariant, non linear, monotonically increasing relationship should exist between the intensities of two images. Karel. et. al [14] combine the approaches of [16] and [17] and attempts to give a general and fully automatic method of correcting intensity loss in CLSM images. The proposed method manipulates the image histogram as in Karel. et. al [14], but it focuses on a continuous domain of probabilities to filter the foreground information to calculate the correction parameters. Before we present our approach, some background on Karel. et. al [14] is presented in the next section.

3.3 Background of Proposed Work

The approach taken in Karel. et. al [14] consists of two stages. In the first stage, a standard histogram is constructed with the help of histograms of optical sections in the image stack. In the second stage, the individual histograms are warped according to the standard histogram to achieve the brightness and contrast of the standard histogram. The construction of standard histogram is adopted from [18]. The approach is based on landmarks chosen in the image histogram. The landmarks chosen are the minimum and maximum intensities and percentiles of the second mode of the image.

There are 2 types of histograms.

1) unimodal (one mode) , 2) multimodal (more than one mode).

Of the two types, unimodal and bimodal image histograms are observed for CLSM images. With unimodal histogram, the mode usually corresponds to the background. Hence a specific landmark has to be selected apart from the mode to identify the object of interest. In case of bimodal histograms, the second mode corresponds to the main foreground object. Hence it is selected as base for calculating other landmarks in histogram. [14, 18] concentrate on bimodal histogram since medical images produced bimodal histograms. The disadvantage of method [14] is that, no definite method is followed to calculate the second mode which is the basis for setting the scale for the construction of standard histogram. The second mode is calculated by removing the background mode by threshold. The overall mean intensity of the image is set as the threshold. The choice of the actual landmark configuration is an important factor. This mode based method is not appropriate for several applications. Another better approach suggested in [18] is to choose the median of the histogram of the foreground as the landmark. This method also does not guarantee best fit mode in all cases [18]. Apart from the second mode, minimum and maximum intensities are also set as landmarks in the creation of standard histogram. These minimum and maximum intensity landmarks are highly sensitive to noise. In order to eliminate the influence of noise concentrated around minimal and maximal intensity values, the upper and lower boundaries of the standard histogram must be set which requires a lot of interaction with the user. The proposed method aims to overcome the disadvantages of [14] and at the same time correct the intensity loss in photobleached images. The main idea is to filter the foreground information from a given image by modeling it as a mixture of Gaussians

and use this information to compensate the intensity loss of the photobleached images. The mean intensityμ and variance σ^2 of foreground and background image is calculated using Gaussian mixture model. The calculated parameters are used to transform the pixel intensity of photobleached image relative to the intensity of reference image. The following section explains our approach.

3.4 De-photobleaching Approach

In many statistical applications, Gaussian mixture model is used as a general tool for modeling large heterogeneous population. It is a semi parametric estimation approach that provides good flexibility and precision in modeling the statistics of unlabelled (unclassified) sample data. In our case the image data can be assumed to be generated from two components (subpopulation). One is the subpopulation of image data forming the background of the image and the other is the one pertaining to the foreground of the image, but we do not know which observation (image data point) belongs to which component and hence we have missing data. Each component has its own parameters θ, which define the probability density function $P_i(X_n)$ (The probability density function gives the probability of an image data point or pixel X_n [n=1,2,…N] belonging to subpopulation *i*). Expectation Maximization (EM) algorithm is the widely used approach to solve the problem of unknown membership of data otherwise called as missing data. It devises appropriate parameters for the chosen model with respect to the data points generated by individual components. In the EM algorithm, we assign some initial estimates for the parameters. These estimates can be chosen arbitrarily, but their selection will affect the final results. The estimation process consists of two steps, the

Expectation (E) step and the Maximization (M) step. In the expectation step, the expected value of the missing data is calculated. In the Maximization step, the resulting value of the expectation is maximized by selecting new parameters according to the direction of the gradient. The E and M steps are iterated until a stopping criterion such as a predefined number of iterations or until there is no change in the mixture model parameters.

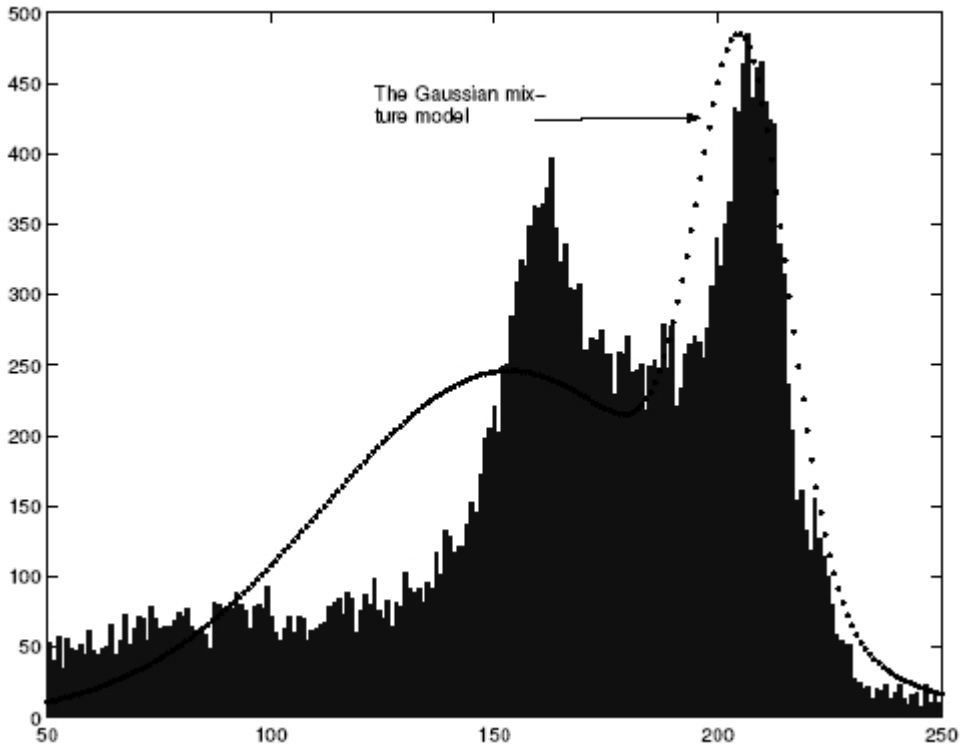

Figure 3.2 Component Gaussian Mixture Model:
Comparison of Original Data and Gaussian Model [20]

Most of our application images are bimodal. Hence we concentrate on modelling the image data based on two component Gaussian mixture model shown in figure 2 (the two components are foreground data and background data). Based on the

assumption that the effect of photobleaching increases relatively with time or depth or both, we consider the first image of the stack as the reference image. The reference image has good visual information of the object or specimen which is studied. Initially mean intensity and standard deviation (parameters of Gaussian) are calculated by solving Gaussian mixture model using EM algorithm. Then the parameters of the foreground component are used for warping the each pixel intensity of the image to its relative reference intensity. The same approach can be extended to unimodal image histograms by making minor changes in calculating the mean intensity of the image. The algorithm has two stages 1.calculation of parameters, mean intensity and standard deviation 2.Image Warping. The steps to be followed for both the stages are elucidated below [20][21] .

3.4.1. Determination of Mean Intensity and Standard Deviation:

The two component Gaussian mixture model is solved by EM to determine six unknown parameters

$$\Theta = (p_1, p_2, \mu_1, \mu_2, \sigma_1, \sigma_2)$$

where

p_1, p_2 are mixture weight constants,

μ_1, μ_2 are mean intensities,

and σ_1, σ_2 are standard deviations corresponding to foreground and background distributions, respectively.

Repeat the steps given below for every optical section in the stack until its μ_1 and μ_2 converge.

a) Calculate the pdf P(X_n) (probability density function) for all pixels based on (μ_1, σ_1) and (μ_2, σ_2) respectively.

$$P_i(X_n) = \frac{\exp\left\{-(X_n - \mu_i)^2 / 2\sigma_i^2\right\}}{\left(\sigma_i\sqrt{2\pi}\right)} \qquad 1 \le i \le 2 \qquad (1)$$

b) Estimation step: estimate the probability of membership F(x) for each pixel value in the Gaussian distribution.

$$\mathrm{F}_i(X_n) = \frac{\mathrm{p}_i \times \mathrm{P}_i(X_n)}{\left[\mathrm{p}_1 \times \mathrm{P}_1(X_n) + \mathrm{p}_2 \times \mathrm{P}_2(X_n)\right]} \qquad 1 \le i \le 2 \qquad (2)$$

c) Maximization step: recompute the estimates of the distribution parameters

$$\text{Mixture weight constant } \mathrm{p}_i = \frac{1}{\mathrm{N}} \sum_{\mathrm{n}=1}^{\mathrm{N}} \mathrm{F}_i(X_n) \qquad 1 \le i \le 2 \qquad (3)$$

$$\text{Mean Intensity } \mu_i = \frac{\sum_{\mathrm{n}=1}^{\mathrm{N}} \mathrm{F}_i(X_\mathrm{n}) \times X_\mathrm{n}}{\sum_{\mathrm{n}=1}^{\mathrm{N}} \mathrm{F}_i(X_\mathrm{n})} \qquad 1 \le i \le 2 \qquad (4)$$

$$\text{Variance } \sigma_i^2 = \frac{\sum_{\mathrm{n}=1}^{\mathrm{N}} \mathrm{F}_i(X_\mathrm{n}) \times (X_\mathrm{n} - \mu_i)^2}{\sum_{\mathrm{n}=1}^{\mathrm{N}} \mathrm{F}_i(X_\mathrm{n})} \qquad 1 \le i \le 2 \qquad (5)$$

where

X_n is the image intensity for the n^{th} pixel and

N is the total number of pixels in the image.

The mean intensity and standard deviation are calculated for all the images in the stack. The mean intensity μ and standard deviation σ of the reference image are named as μ_{ref} and σ_{ref} respectively.

3.4.2. Image Warping:

The individual images are transformed to achieve as uniform as possible contrast and brightness of the reference image.

$$X_n' = \frac{(X_n - \mu_1^j) \times \sigma_1^{ref}}{\sigma_1^j} + \mu_1^{ref} \qquad 2 \le j \le K \qquad (6)$$

where

X_n' is the warped intensity of n^{th} pixel of image j,

X_n is the original intensity of pixel of image j,

μ_1^j is the foreground mean intensity of image j,

σ_1^j is the standard deviation of image j,

μ_1^{ref} is the foreground mean intensity of reference image,

σ_1^j is the standard deviation of reference image,

and K is the total number of images in the image stack

3.5 Experimental Results

The proposed approach was implemented in Matlab and tested on several sets of images in Biovision lab database. The experimental image sequences were acquired by Zeiss LSM 510 META laser scanning confocal microscope. The image size is (512 x 512), and image sequences were taken about 1 frame per 1.3 second, with a length in the range of 160 to 220 frames. The initialization is crucial for Expectation Maximization algorithm. To start, with the mixture weight constants p, mean intensities μ and variance σ^2 are initialized as follows,

$p_1 = p_2 = 0.5$ with ($p_1 + p_2 = 1.0$),

μ_1= mean intensity of the image/2,

$\mu_2 = 3 \times \mu_1$,

and $\sigma_1^2 = \sigma_2^2$ = variance of the image/4

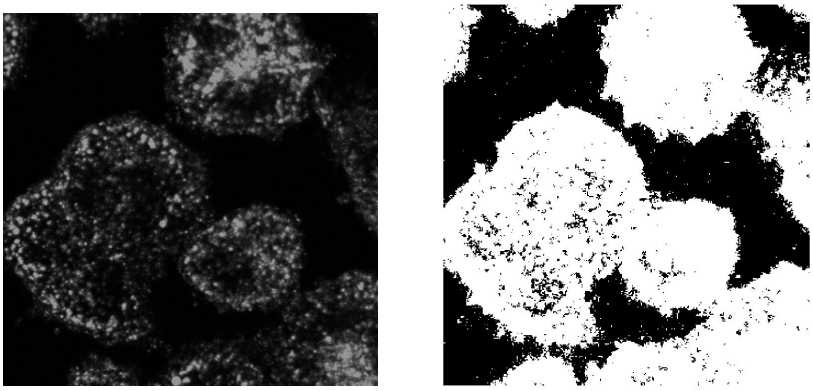

(a) (b)

Figure 3.3 Foreground differentiated from the background of an image:
(a) Original Image (b) Filtered Image (white region denotes foreground and black region denotes background)

The performance of the algorithm is improved by using parameters (p, μ, σ^2) of previous optical section as initialization for the next optical section calculation. Figure 3.3 depicts the filtered foreground information of an optical section in the stack which is obtained at the end of stage one of the EM algorithm. The white region is the foreground object and the black region corresponds to the background of the image. In Figure 3.4, we show the original photobleached images (numbered from top to bottom of image stack 1). The entire stack was processed by our algorithm using Figure 3.4 (a) as the reference image. Figure 3.5 (a) shows the histogram of the reference image. Figure 3.5 (b) and 3.5 (c) show the histogram of optical section 220 before and after correction. The corrected image 220 has a visual contrast similar to that of its reference image. From figure 3.5 (a) and 3.5 (b), we could see a vast difference between the mean intensities of optical section 1 and 220 of the original image stack. The corrected image 220 in Figure 3.5 (c) has mean intensity close to its reference image intensity (Figure 3.5 (a)). From figure 3.6, we can see the intensity drops steadily with increasing optical section number. The proposed method has helped to maintain a constant intensity for the entire stack. In Figure 3.7, we could observe that the mean intensities of the foreground object of the stack is uniform with very little fluctuations. Though there is an increase in the intensity of background object, it is of negligible value. Figure 3.9 and 3.11 shows another set of images (image stack 2) acquired by confocal microscope before and after correction. From Figure 3.10, we could observe that original mean intensity curve of foreground does not dip as expected according to properties of photo bleaching effect. Hence we could assume other factors such as signal to noise ratio,

geometrical optics played a role for the loss in intensity of the images. Our approach has produced good results even for such images (Figure 3.10). Thus the experimental results demonstrate that the proposed method can be used as a good tool to correct the intensity loss in photobleached images.

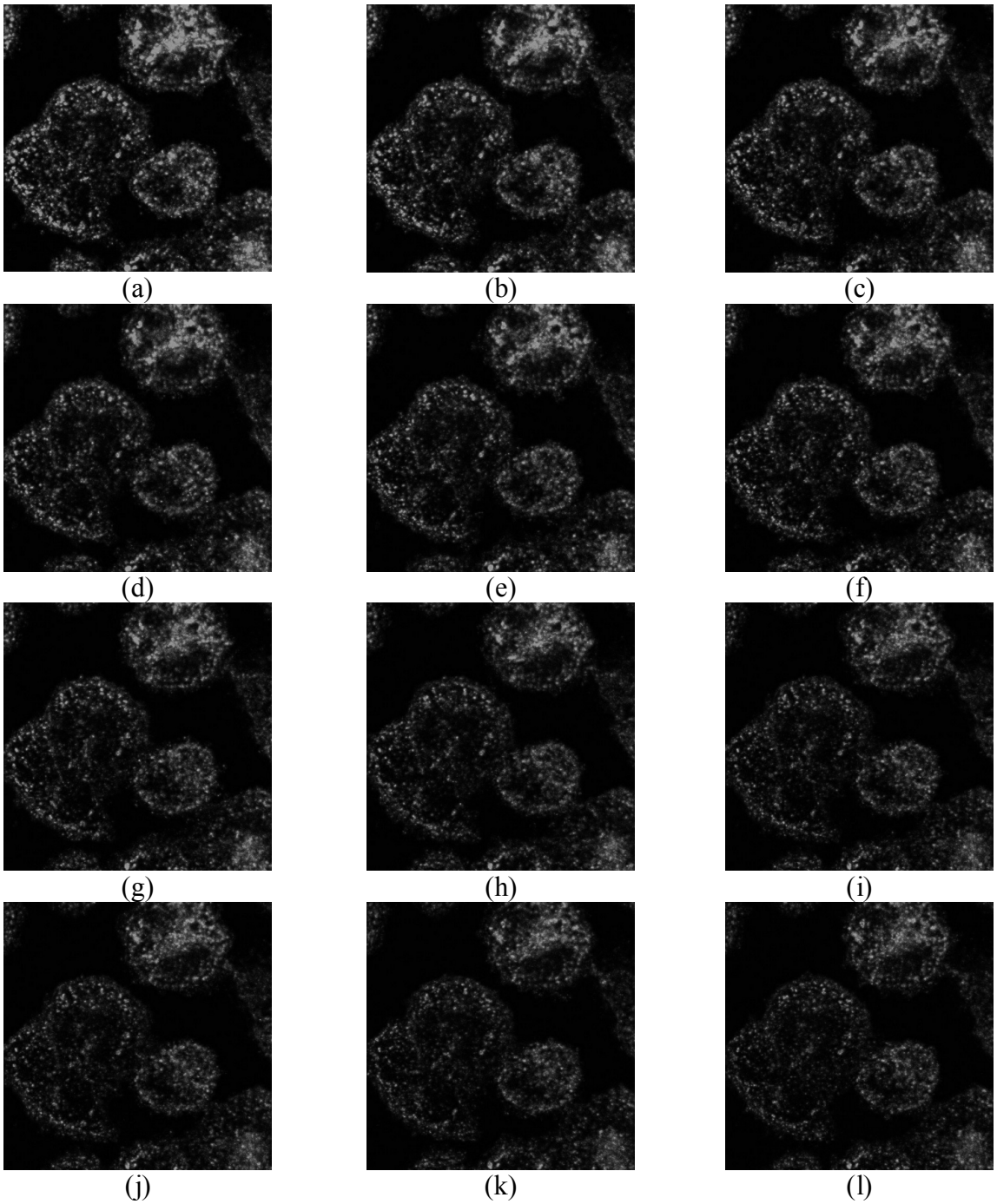

Figure 3.4 Reference section # 1 and some sections from original image stack 1 Sections: (a) #1 (b) #20 (c) #40 (d) #60 (e) #80 (f) #100 (g) #120 (h) #140 (i) #160 (j) #180 (k) #200 (l) #220

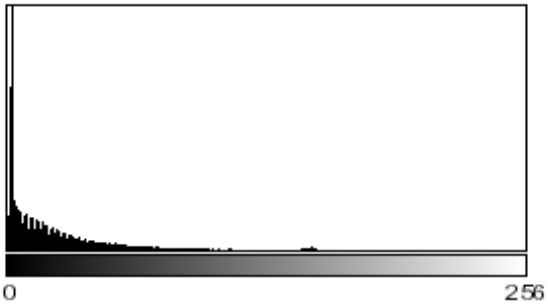

(a)

(b)

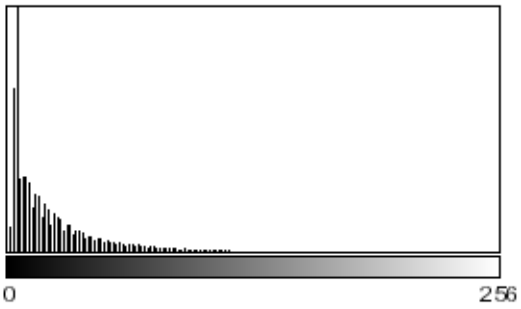

(c)

Figure 3.5 Image Histogram of Image Stack 1: (a) Reference Image (b) Original Image #220 (c) Restored Image #220

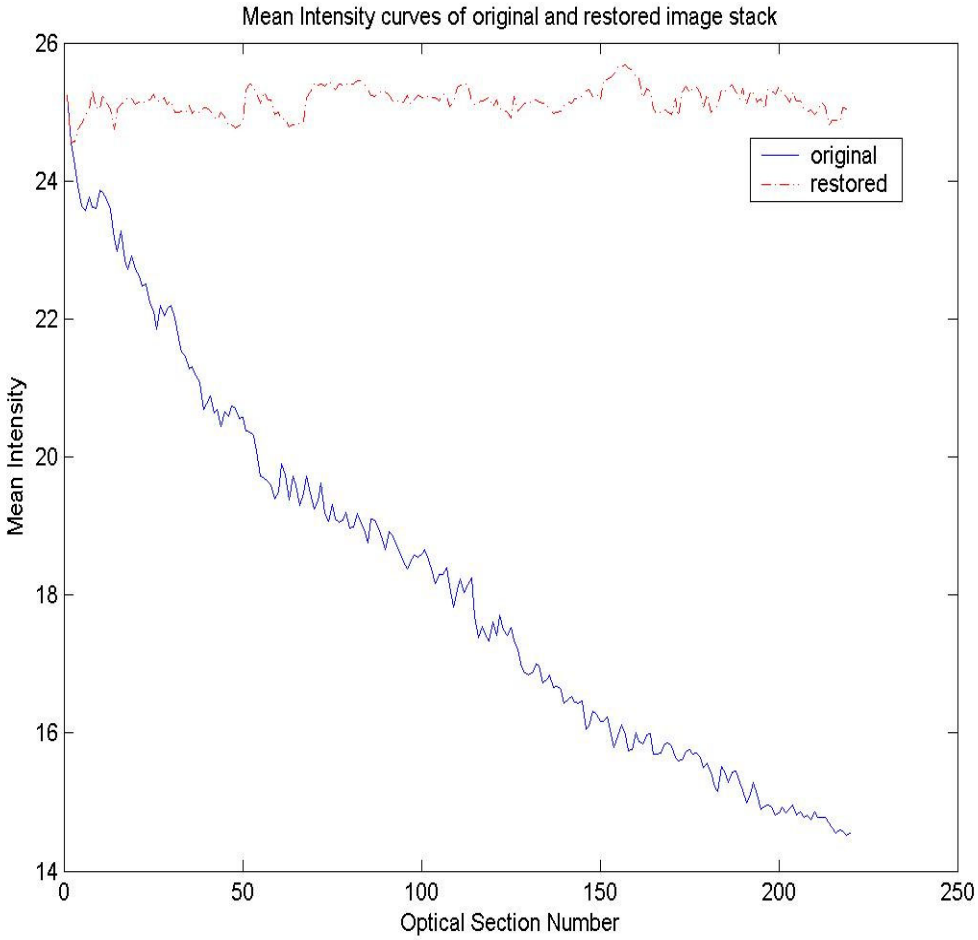

Figure 3.6 Mean Intensity Curve of Image Stack 1

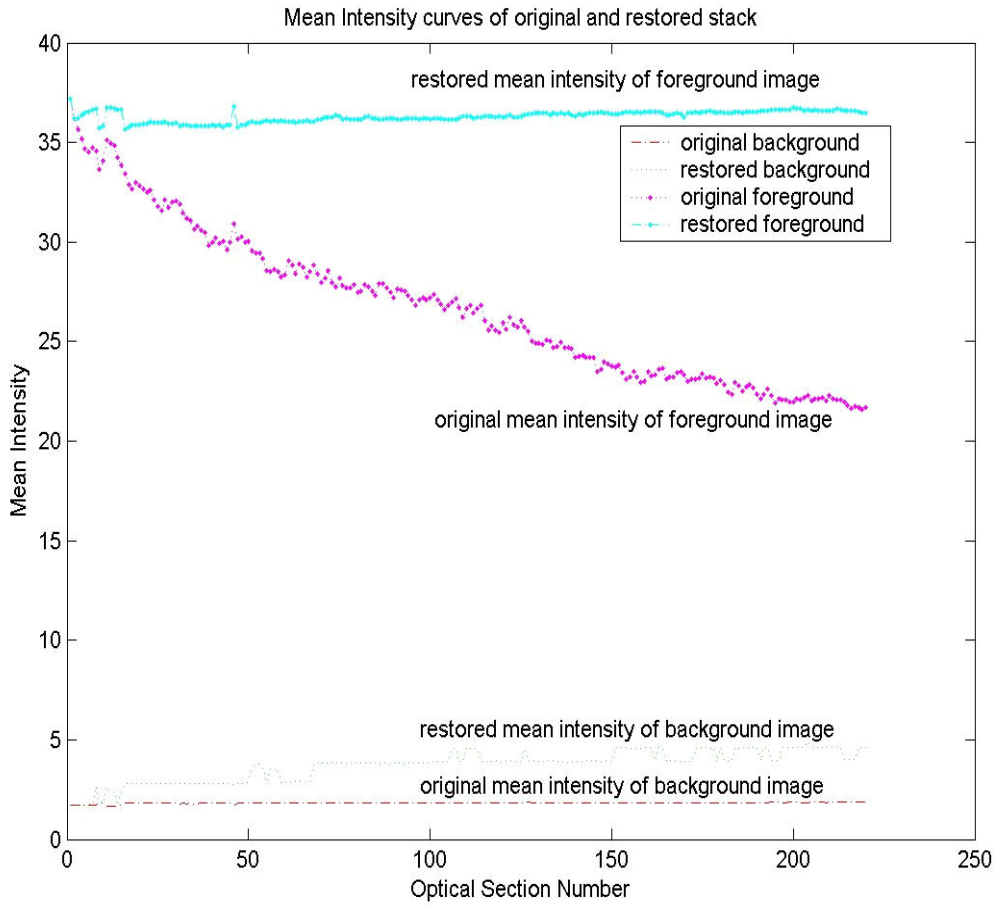

Figure 3.7 Mean Intensity Curve of Background and Foreground (image stack 1)

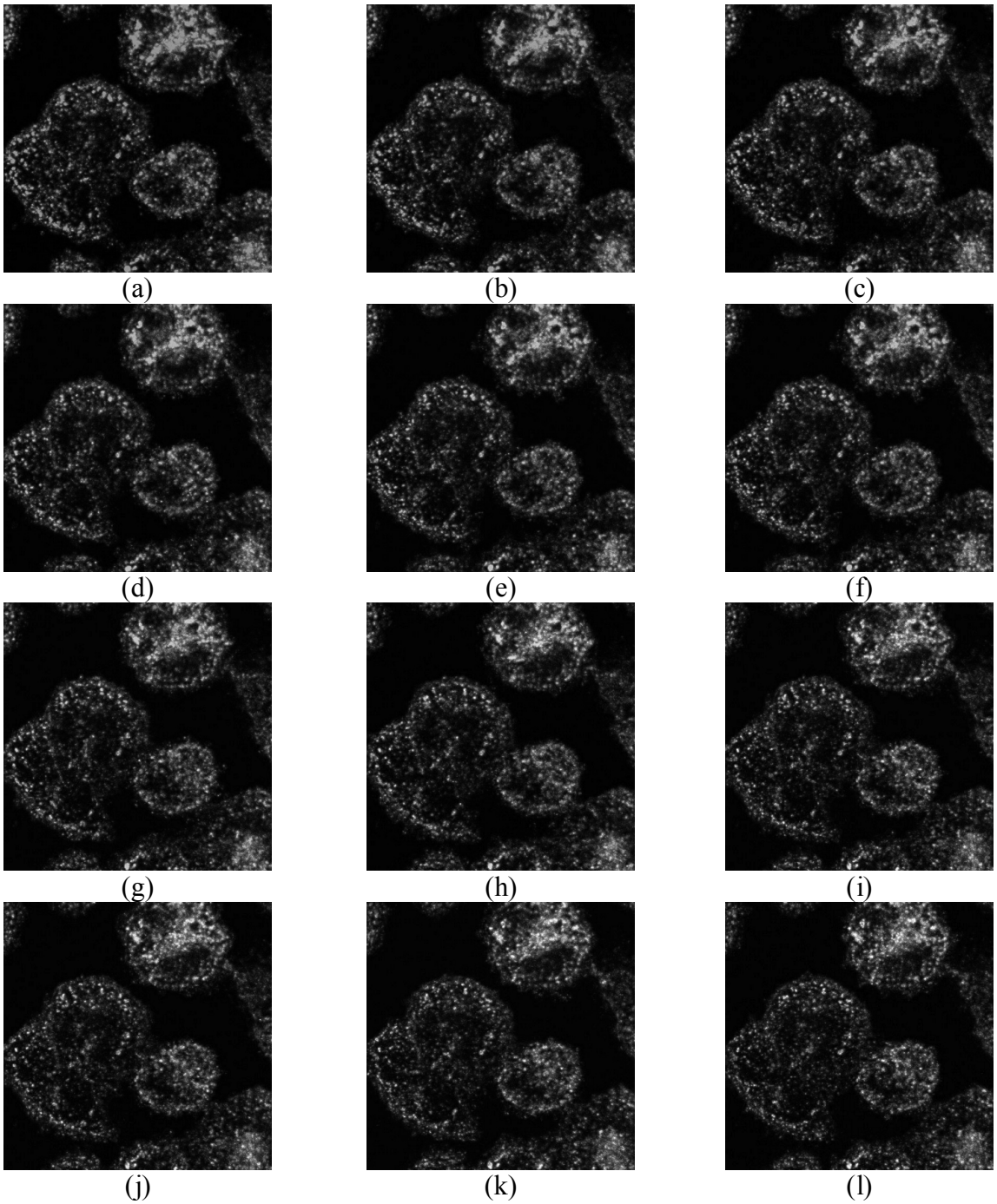

Figure 3.8 Reference section # 1 and some sections from restored image stack 1 Sections: (a) #1 (b) #20 (c) #40 (d) #60 (e) #80 (f) #100 (g) #120 (h) #140 (i) #160 (j) #180 (k) #200 (l) #220

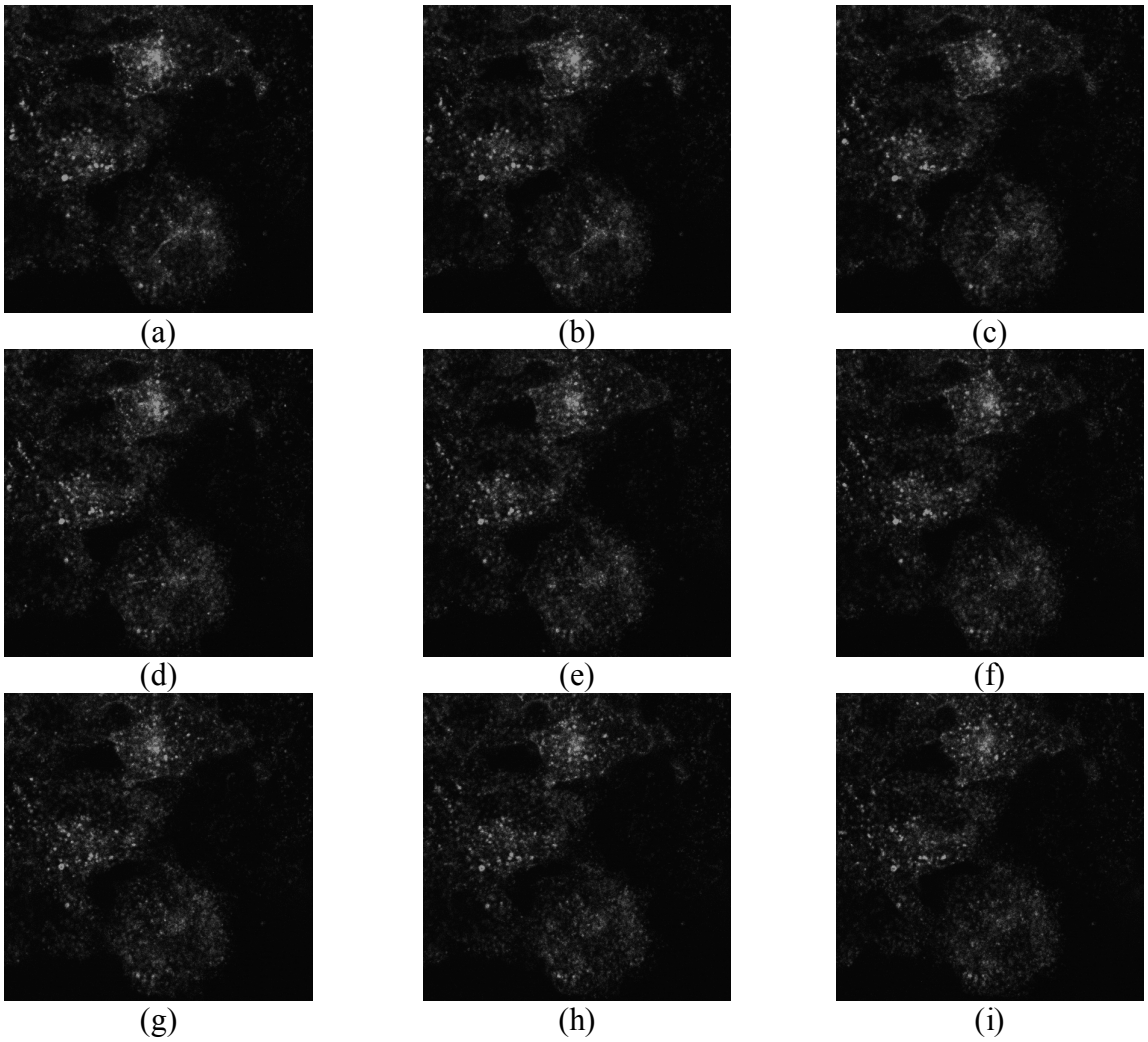

Figure 3.9 Reference section # 1 and some sections from original image stack 2
Sections: (a) #1 (b) #20 (c) #40 (d) #60 (e) #80 (f) #100 (g) #115 (h) #130 (i) #166

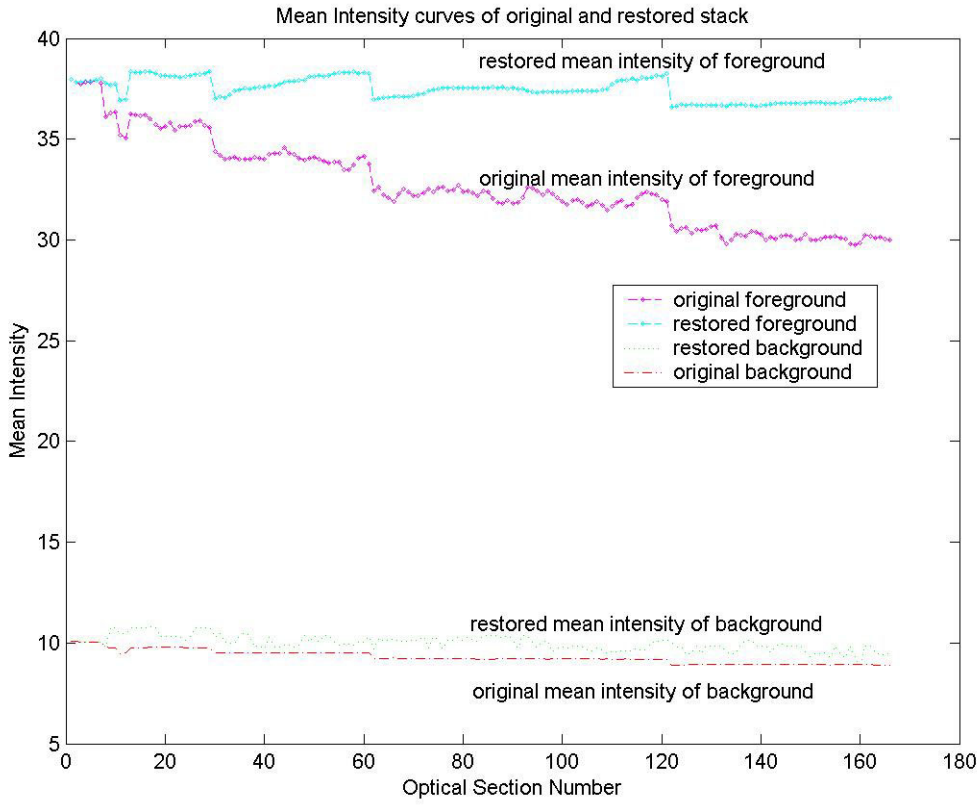

Figure 3.10 Mean Intensity Curve of Background and Foreground (image stack 2)

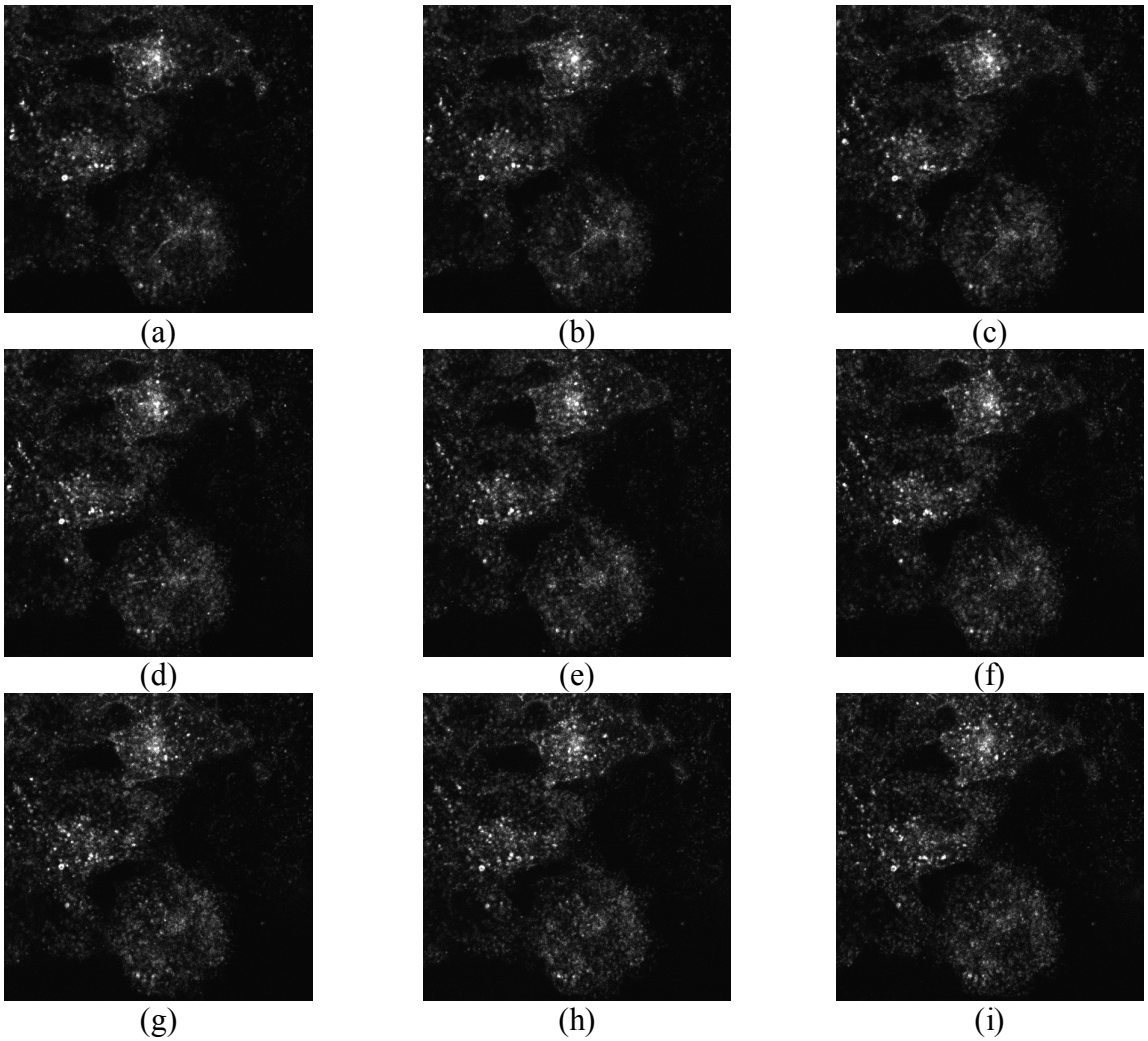

Figure 3.11 Reference section # 1 and some sections from restored image stack 2
Sections: (a) #1 (b) #20 (c) #40 (d) #60 (e) #80 (f) #100 (g) #115 (h) #130 (i) #166

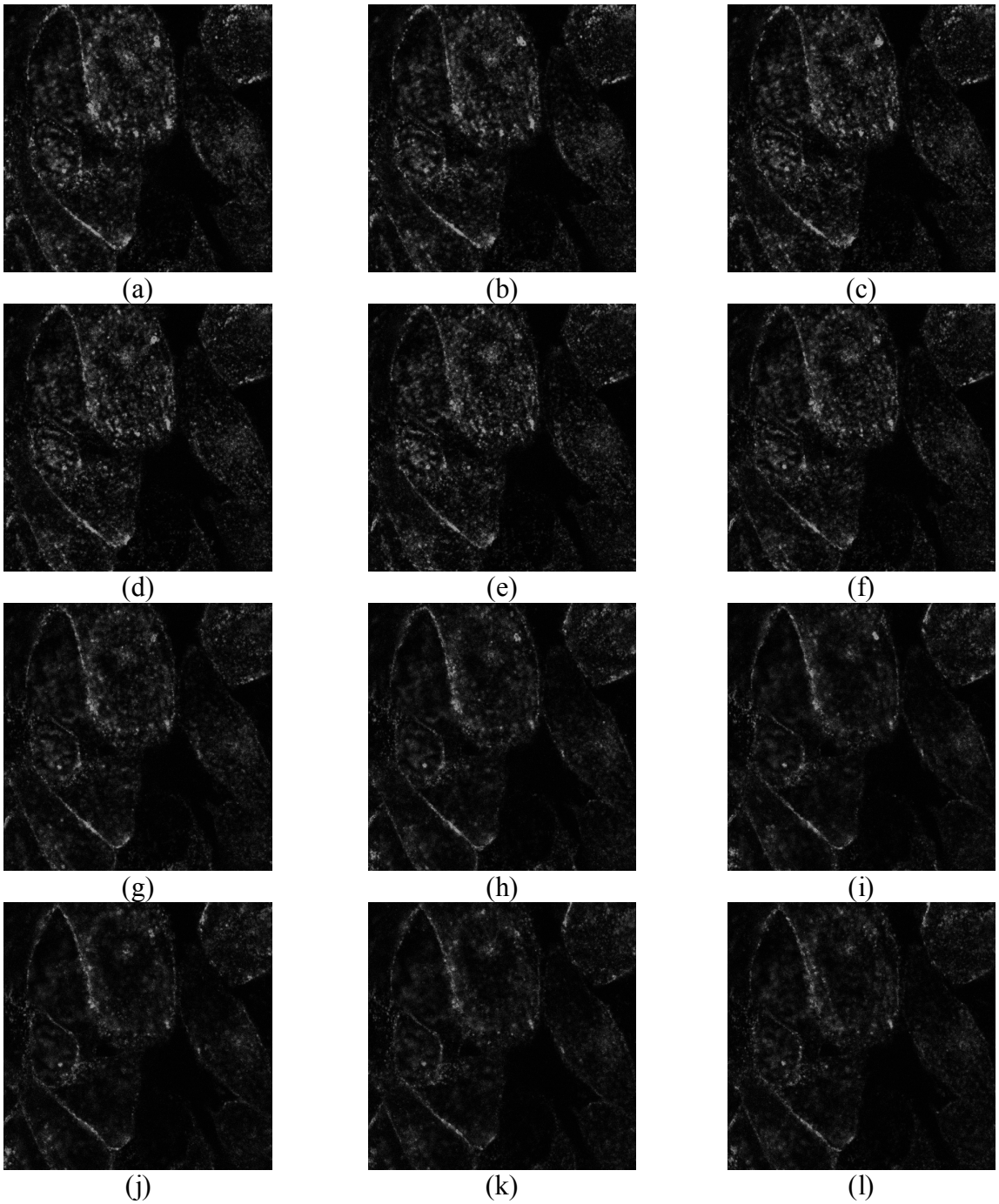

Figure 3.12 Reference section # 1 and some sections from original image stack 3 Sections:(a) #1 (b) #20 (c) #40 (d) #60 (e) #80 (f) #100 (g) #120 (h) #140 (i) #160 (j) #180 (k) #200 (l) #220

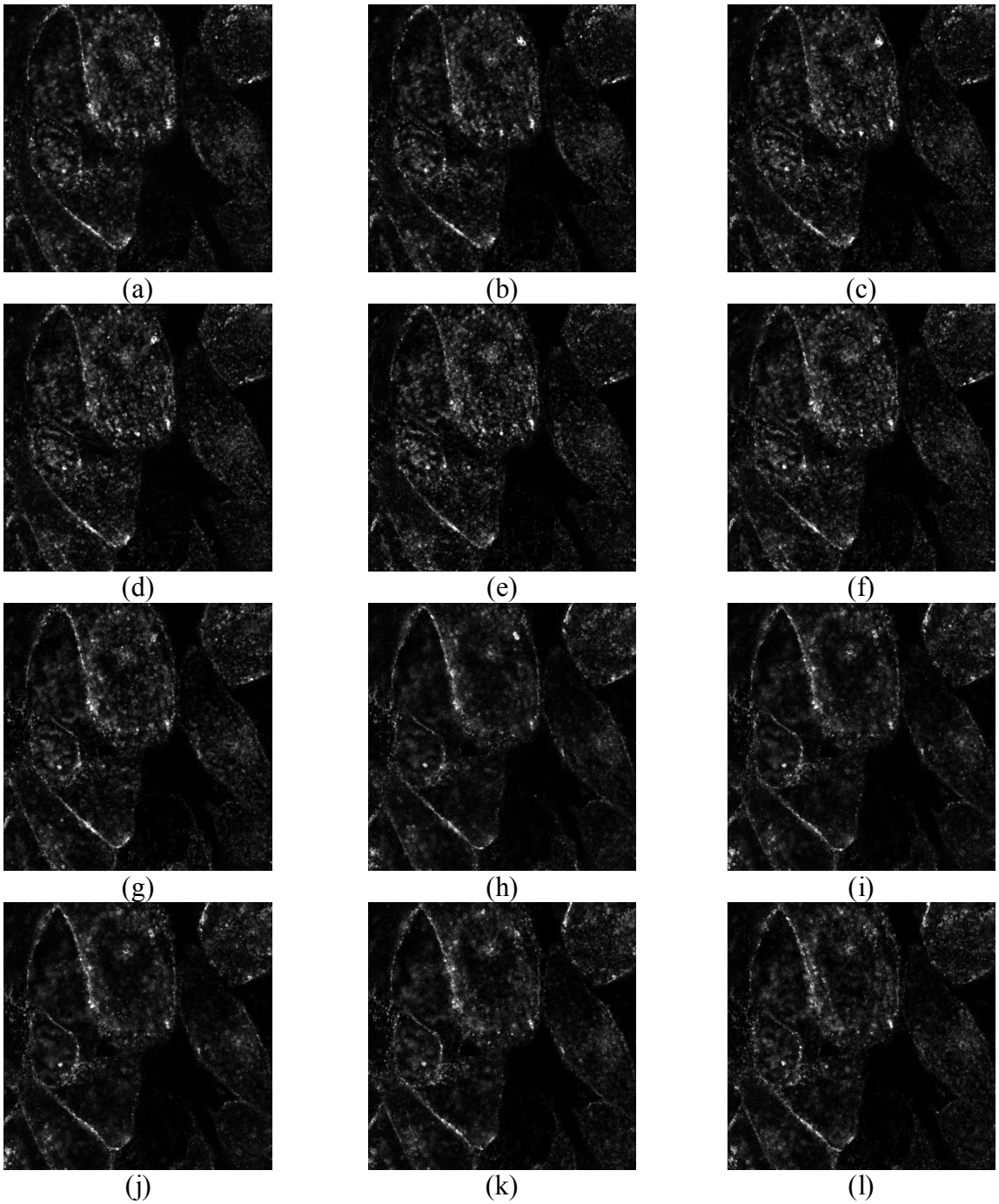

Figure 3.13 Reference section # 1 and some sections from restored image stack 3 Sections: (a) #1 (b) #20 (c) #40 (d) #60 (e) #80 (f) #100 (g) #120 (h) #140 (i) #160 (j) #180 (k) #200 (l) #220

CHAPTER 4

DESIGN PRINCIPLES OF ICellDAS INTERFACE

The objective of IntraCellular Dynamic Analysis System (ICellDAS) is to develop an online image processing service. The success of any Web based service attributes to one important factor is Interface design. This paper reports on the philosophies, principles followed while designing the interface for ICellDAS. Section 4.1 talks about user interface design principles. Section 4.2 contains the techniques that are to be followed while developing a user interface. The chapter ends with a brief introduction to the various tools used in the development of ICellDAS in section 4.3.

4.1 User Interface Design Principles

The general principles of interface design are heuristic. They are more in the nature of rules of thumb than specific usability guidelines. The following principles are fundamental to the implementation of effective interface, whether for traditional GUI environments or the web [22] [23] [24].

1. Principle of structure: The user interface must always be designed based on clear, consistent models that are recognizable to users. The interface should be organized in such a manner that the user is able to make clear distinction of a group of related items and items that do not fit in a group. The structure principle is concerned with the overall user interface structure.

2. Principle of simplicity: The design should speak the user's language. It should use words and concepts familiar to user. It must enable user to perform common tasks with very little or no effort.
3. Principle of visibility: The design should not have any extraneous or redundant information. At the same time there should be sufficient options and material to complete a chosen task. The user should not have to remember information from one part of the dialogue to another. Instructions for use should be visible or easily retrievable whenever appropriate.
4. Principle of feedback: The design should always keep the user informed of actions or interpretations, changes of state or condition and errors or exceptions that are relevant to the user in a clear, concise and unambiguous language. For instance in ICellDAS, the user has to select one of the thumbnail images from more than hundred to perform image analysis on it. From the human vision point of view, all the images look alike and there are chances that the user might get confused while selecting his desired image based on time scale or z-axis scale. To avoid any confusion, as soon as the user selected the thumbnail image from the image frame, the selected image is highlighted and sufficient information is given in the image label. This is shown in Figure 4.1
5. Principle of tolerance: The design should expect users to make errors and anticipate where they will go wrong. It should be flexible enough to accept varied input and provide options for easy reversal of actions.

6. Principle of reuse: The design should reuse internal and external components and behaviors, maintaining consistency with purpose rather than providing arbitrary consistency.
7. Principle of aesthetics: It is not necessary that each web page be a visual work of art. But it is important that it not be ugly. The pages of ICellDAS are simple and elegant with no extra information or designs which will deviate the user's attention from his/her objective to study and analyze the images. Figures 4.2 and 4.4 show the simple design of ICellDAS 2D and 3D pages.

4.2 User Interface Design Techniques

Clever code or applying an interesting color scheme is not sufficient to bring out the advantages of a good interface. The interface design must meet the expectations of diverse user groups from a novice user who needs helps at every step to frequent users wanting to get where they want as quickly as possible. Interface designers over the years have learned and given few valuable techniques that could help achieve a good interface design. The following tips were followed while designing the ICellDAS user interface [22] [23] [24].

1. Consistency: consistency in user interface enables users to build an accurate mental model of the way it works, and accurate mental model leads to lower training and support costs. Modeling Standards should be applied in all aspects of software development, including user interface design. To maintain consistency, all the navigation buttons and menus are designed to feel alike and perform same functions in all the pages of ICellDAS.

2. Navigation: The application will make sense to the users only if the flow between screens matches the flow of work the user is trying to accomplish. User interface flow diagrams help in the understanding of flow of user interface.
3. Effective Wording: The text which is displayed on screen is the primary source of information to the users. Using full words and sentences, as opposed to abbreviations and codes helps user to grasp information easily. Identical terminology is used in prompts, menus and help screens of ICellDAS. Apart from text, symbols are used where ever necessary to help user understand different operations easily. For instance the navigation buttons such as next and back contains appropriate arrows to help the user understand the purpose of those buttons.
4. Appropriate colors: Colors must be chosen such that it makes the interface appealing to the user's eyes. The colors must be selected based on the contrast rule which states that dark colored text should be placed on light colored background and vice versa.
5. Expect users to make mistakes: A good design prevents a problem to occur in the first place. The error prone conditions must be eliminated or checked with a confirmation of the user before it is committed to action. The interface must be designed to recover from user errors with less effort and time. The ICellDAS pages are carefully designed so that the user makes no errors. For instance, if the user performs a wrong operation, say he/she intended to crop a different part of

image, then he/she can readily get back the original image by just clicking the reset button on the interface.

6. No crowded user interface: Crowded interface are difficult to understand and hence difficult to use .Experimental results show that the overall density of the screen should not exceed 40 percent, where as local density within the groupings should not exceed 62 percent. There are hundreds of images which have to be presented to the ICellDAS users. In order to avoid clutter, each page is designed to carry not more than 100 images. This also makes download time of each page bearable.
7. Group effectively: Items that are logically connected should be grouped together on the screen to communicate they are related, whereas items that have nothing to do with each other should be separated. Hundreds of images which are to be presented to ICellDAS user are grouped effectively. Sufficient details are provided in form of text messages to help user identify each image based on time scale. All information regarding a particular type of image is grouped effectively. For instance the tracking of single particle is displayed as an animation in a child window, so that the user can visualize the dynamic version of tracking instead of just getting the end result trajectory path. This is depicted in Figure 4.3

4.3 Tools Used for ICellDAS Development

ICellDAS algorithms are implemented in Java language and the dynamics of user interface screens is done by JavaScript. The reason for choosing Java technology for development of ICellDAS is elucidated below.

Image processing is of central importance to the web. Images are the most widely used data format in the web. Java appears to be the most suited language for image processing in the web [25]. The Image processing programs are portable due to Java Virtual Machine (JVM). The compile once run-anywhere advantage of java helps the developer not to depend on expensive workstations or a single development platform to distribute the image processing algorithms. Browsers are growing in size and complexity. Hence it is expected to install plug-ins and helper applications that enable decoding of growing number of image formats. Java obviates the need for deployment of distended browsers and helper applications that congest our computing environments.

JavaScript, a derivative of Java is used to create interactivity on the client side webpage of ICellDAS. No special software is required to be installed on the part of the user and it has a fast test and modify cycle [26]. It helps to write simple client functions that would other wise require requests for additional pages and/or server side programming. For instance, a simple script is provided to switch from one image to another with very little or no information to be exchanged between the web server and the client page. This increases the speed of that operation. To sum up, JavaScript is well

suited for fast downloading, has minimal security risks and performs well across all types of browsers.

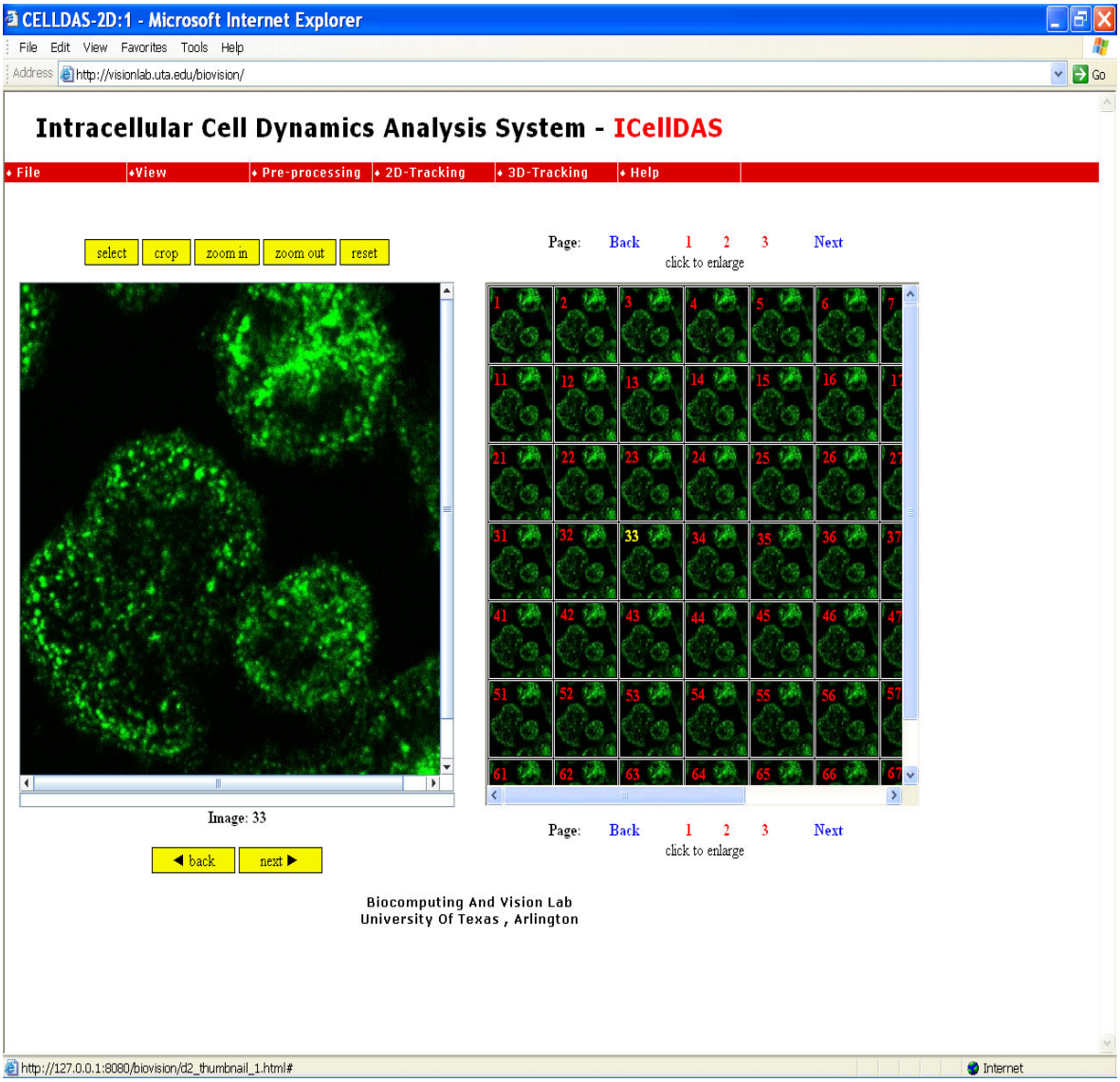

Figure 4.1 Selection of Image Number 33

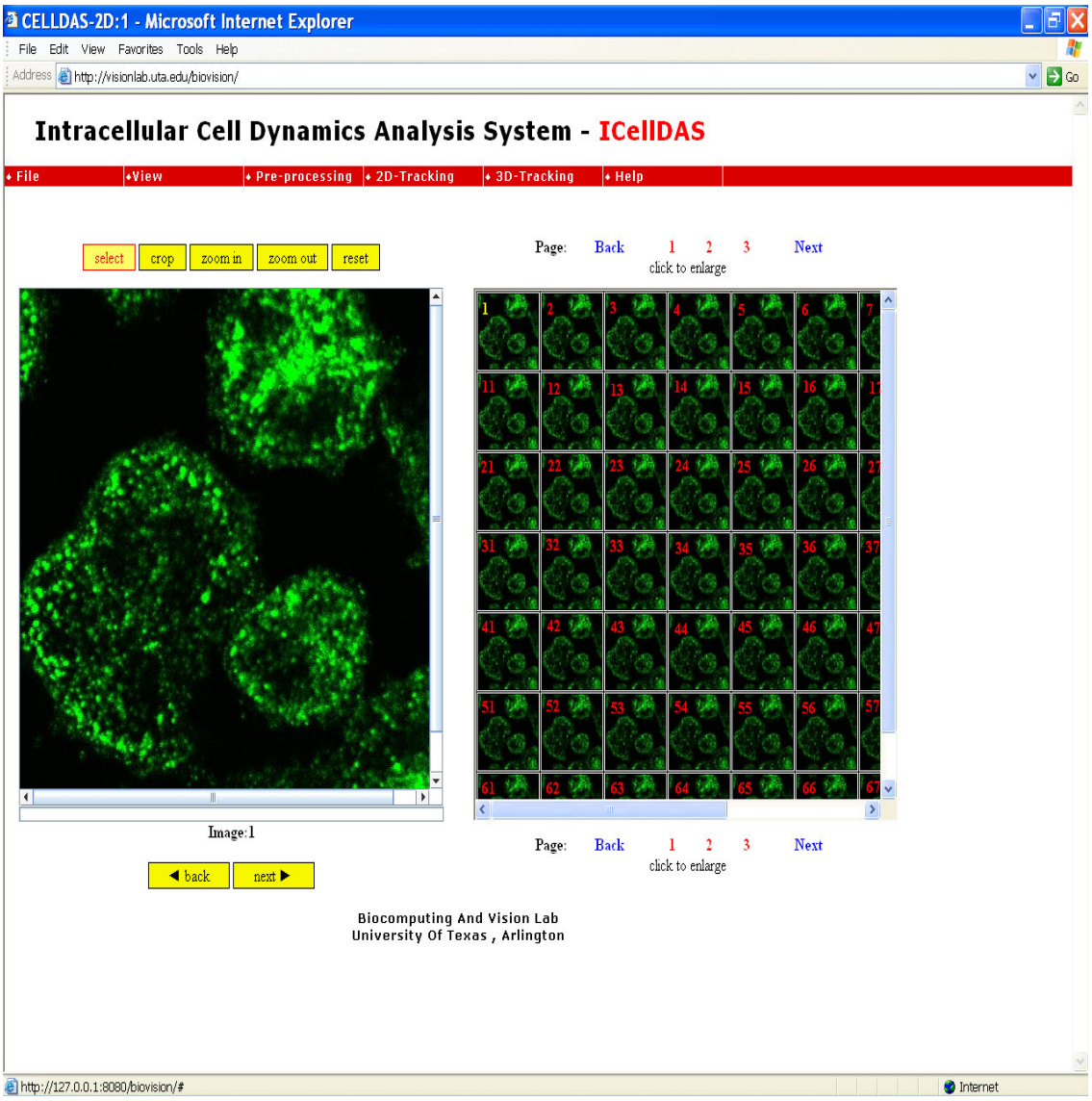

Figure 4.2 Home Page of ICellDAS

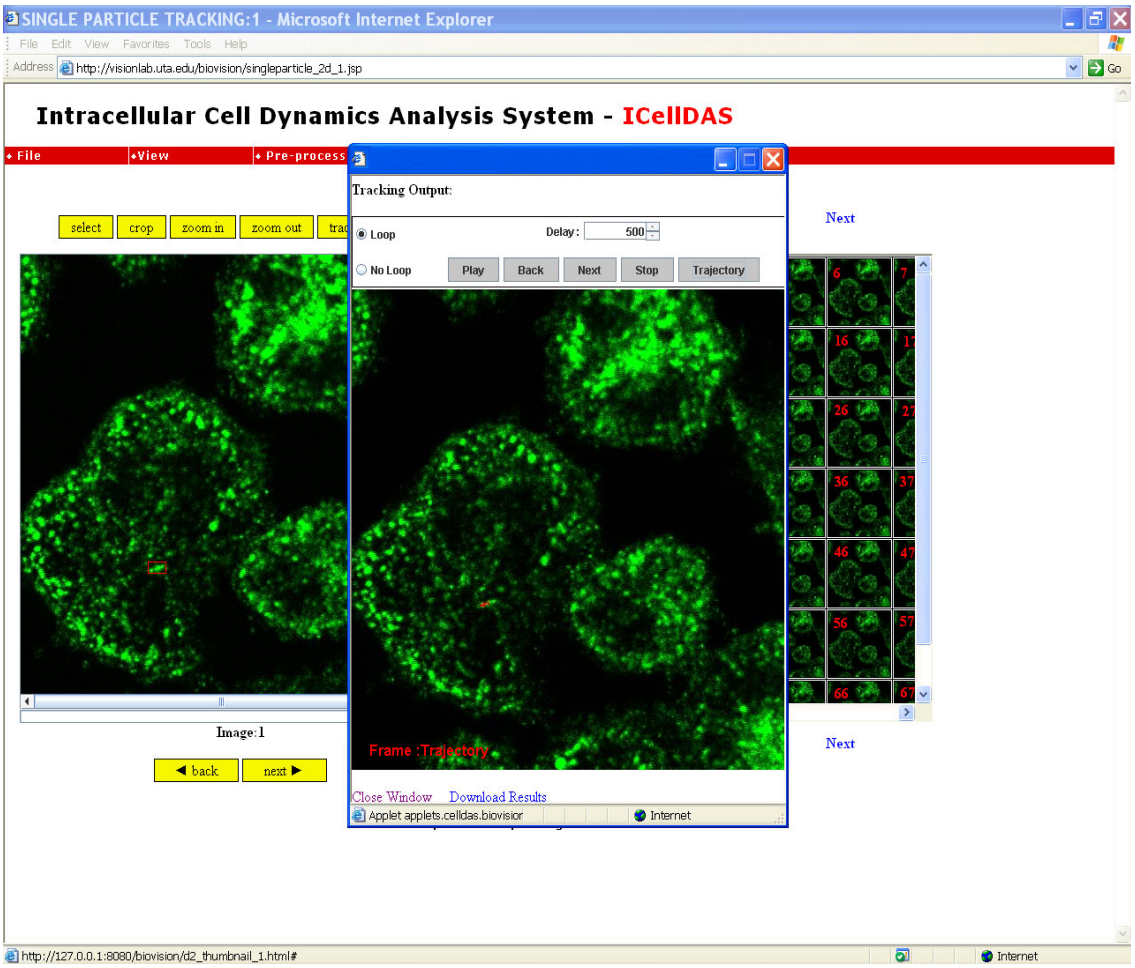

Figure 4.3 ICellDAS-Single Particle Tracking: Animation pop-up window

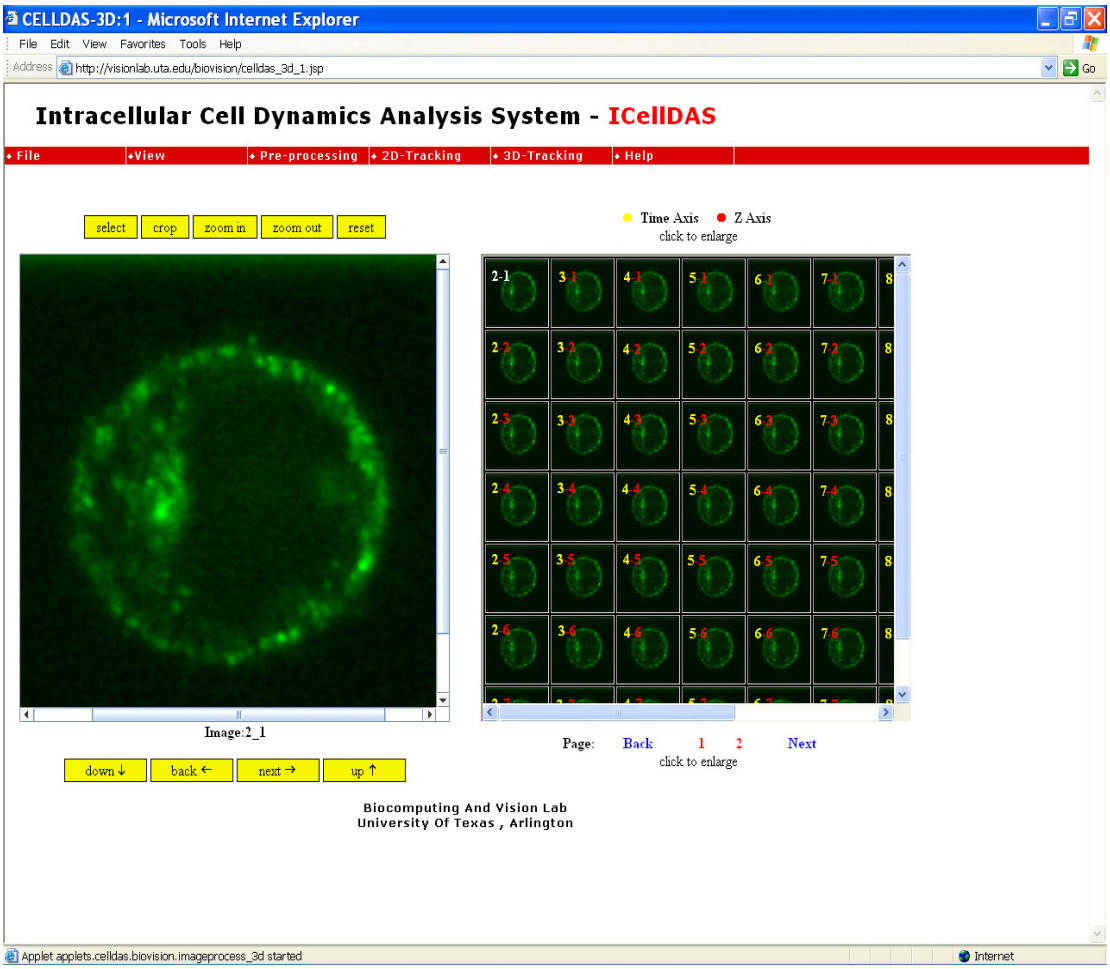

Figure 4.4 ICellDAS 3D Image Page

CHAPTER 5

CONCLUSION AND FUTURE WORK

In this thesis, we have proposed a Gaussian model approach to offset the intensity loss of photobleached images. The approach requires very little user interaction and gives user a possibility to make better analysis of the photobleached image. The corrected images have a better visual contrast and value than the original ones. The approach can also be used as a general tool to compensate the intensity loss due to other factors such signal to noise ratio, geometrical optics; apart from the photobleaching effect. It should be noted that the problem of intensity attenuation is complex and this method does not intend to recover the lost information but provide a better visualization to make analysis easier when compared with using the original image set. In addition to this work, interface for ICellDAS has been developed. Every effort has been taken to follow user design principles and philosophies during the development. The goal of the design is to provide a user friendly web based tool for image analysis. The design has helped to identify various user and program constraints that need to be addressed for the successful launch of ICellDAS as a image processing and analysis tool into the market.

One of the important criteria for a good web based application is speed. The performance of the proposed de-photobleaching algorithm can be improved by K means algorithm, a variant of Expectation Maximization algorithm which classifies the image

data into a certain number of clusters to build a probability model for the data. With regard to ICellDAS interface, a lot of issues such as speed, memory limitations, and security of the images have to be addressed in the future.

REFERENCES

[1] Harry A. Crissman, J. Paul Robinson, *"Methods in Cell Biology,"* Volume 63, third edition, part A, chapter 4, Academic Press publication.

[2] Thomas J. Fellers and Michael W. Davidson, National High Magnetic Field Laboratory,1800 East Paul Dirac Dr, Florida State University, Florida, http://www.olympusflowview.com .

[3] Robert W. Redmond, *"Hand Book of Biomedical Fluorescence,"* Introduction to fluorescence and photophysics, Marcel Dekker Inc, pg 1-29.

[4] Guilbault. G, *"General Aspects of Luminescence Spectroscopy in Practical Fluorescence,"* second edition, Marcel Dekker Inc, pg 1-40

[5] Dr.Thomas G. Chasteen, Department of Chemistry, Sam Houston State University, Huntsville, Texas, http://www.shsu.edu/~chemistry/chemluminescence

[6] Denis Semwogerere, Eric. R. Weeks,"*Confocal Microscopy,"* Encyclopedia of Biomaterials and Biomedical Engineering, DOI : 10.1081/ E-EBBE-120024153

[7] Nathan S. Claxton, Thomas J. Fellers, Michael W. Davidson, Department of Optical Microscopy and Digital Imaging, National High Magnetic Field Laboratory, Florida State University, Florida, *"Laser Scannning Confocal Microscopy"*

[8] Keller H. E, Pawley J. B, Ed .; Objective Lenses for Confocal Microscopy, *"In Handbook of Biological Confocal Microscopy,"* second edition, Plenum Press, New York 1995, pg 111-126

[9] Kino G. S, Pawley J. B , Ed .; Intermediate optics in Nipkow Disk microscopes, *"In Handbook of Biological Confocal Microscope,"* second edition, Plenum Press, New York 1995, pg 155-165.

[10] J. Paul Robinson, Purdue University, Cytometry Laboratories, *"Introduction to Confocal Microscopy,"* Plenum Press, second edition.

[11] Nana Rezai, Pathology, University of British Columbia, *"Taking the confusion out of Confocal microscopy,"* BioTech Journal, April 2003, Volume 1 , pg 75-80.

[12] X. Wu, L. Ji, Department of Automation, Tsinghua University, Beijing, *"Fully automated intensity compensation for Confocal microscopic images"*.

[13] Negahdaripur. S, Yu. C. H,*"A generalized brightness change model for computing optical flow, "*International Conference Computer Vision and Pattern Recognition, June 1994, 593600.

[14] Karel Hana, Paul Smrcka, Martin Capek, Lucie Kubinova, *"Compensation of contrast and brightness attenuation with depth in confocal microscopy,"* ACM publication.

[15] Periaswamy. S, Farid.H, *"Elastic Registration in the presence of intensity Variations,"* IEEE Trans. Med. Imaging, July 2003.

[16] Kevrann. C, Legland. D, Pardini. L ,"*Robust incremental compensation of the light attenuation in 3D fluorescence microscopy,"* The Royal Microscopial Society, Volume 214, June 2004, pg 297-314.

[17] Cox .I. J, Roy. S, Hingorani. S. L,*" Dynamic histogram warping of image pairs for constant image brightness,"* IEEE Int. Cong. on Image Processing, 1995, 0-8186-7310-9/95

[18] Jayaram K.Udupa, Xuan Zhang, Nyul .G, *"New Varaints of a Method of MRI Scale Standardization,"* IEEE Transactions on Medical Imaging, Volume 19, Number 2 February 2000 .

[19] J. Lippincott-Schwarz, et al.,*"Nature Cell Biology,"* 2003, pg 7-14, http://mekentosj.com/science/frap/ .

[20] Shubing Wang, Department of Statistics, University of Wisconsin, Madison, *"Gaussin Mixture Model by Using EM"*.

[21] Petteri Nurmi, *"Mixture Models,"* Helsinki Institute for Information Technology, petteri.nurmi@cs.helsinki.fi

[22] Scott W. Ambler, *"The Object Premier: Agile Model-Driven Development with UML 2.0,"* third edition Cambridge University Press, Chapter 6: User Interface Development, ISBN: 0521540186.

[23] Commodore- Amiga," Amiga User Interface Style Guide ", Addison Wesley Publishing Company, first edition, ISBN: 0201577577.

[24] *"Macintosh Human Interface Guidelines,"* Apple Computer staff, Addison Wesley publication, 1993, ISBN: 0-201-62216-5

[25] Douglas A. Lyon, *"Image Processing in Java,"* Prentice Hall Publication, 1999, pg 5-30

[26] Robert Crooks, Allaire Educational services, http://www.adobe.com/v1/documents/js2/js000.cfm

BIOGRAPHICAL INFORMATION

Sowmya Gopinath received her Bachelor of Engineering degree in Information Technology from Sona College of Technology affiliated to Periyar University, Tamil Nadu, India in 2004. She received her Master of Science degree in Computer Science and Engineering from The University of Texas at Arlington in December 2006.